CCDC92 deficiency ameliorates podocyte lipotoxicity in diabetic kidney disease

Fuwen Zuo, Youzhao Wang, Xinlei Xu, Ruihao Ding, Wei Tang, Yu Sun, Xiaojie Wang, Yan Zhang, Jichao Wu, Yusheng Xie, Min Liu, Ziying Wang, Fan Yi

PII: S0026-0495(23)00328-1

DOI: https://doi.org/10.1016/j.metabol.2023.155724

Reference: YMETA 155724

To appear in: *Metabolism*

Received date: 10 August 2023

Accepted date: 3 November 2023

Please cite this article as: F. Zuo, Y. Wang, X. Xu, et al., CCDC92 deficiency ameliorates podocyte lipotoxicity in diabetic kidney disease, *Metabolism* (2023), https://doi.org/10.1016/j.metabol.2023.155724

CCDC92 deficiency ameliorates podocyte lipotoxicity in diabetic kidney disease

Fuwen Zuo[1], Youzhao Wang[1], Xinlei Xu[1], Ruihao Ding[1], Wei Tang[2], Yu Sun[1], Xiaojie Wang[1], Yan Zhang[1], Jichao Wu[1], Yusheng Xie[1], Min Liu*[1], Ziying Wang*[1] and Fan Yi*[1,3]

[1]Department of Pharmacology, School of Basic Medical Sciences, Shandong University, Jinan, 250012, China.
[2]Department of Pathogenic Biology, School of Basic Medical Sciences, Shandong University, Jinan, 250012, China
[3]National Key Laboratory for Innovation and Transformation of Luobing Theory, Key Laboratory of Cardiovascular Remodeling and Function Research, Chinese Ministry of Education and Chinese Ministry of Health, Qilu Hospital, Shandong University, Jinan, 250012, China.

*** Correspondence:**
Fan Yi, Department of Pharmacology, School of Basic Medical Sciences, Shandong University, Jinan, 250012, China. Tel: 86-531-88382616, Fax: 86-531-88382616, Email: fanyi@sdu.edu.cn;
Ziying Wang, Department of Pharmacology, School of Basic Medical Sciences, Shandong University, Jinan, 250012, China. Tel: 86-531-88382036, Fax: 86-531-88382036, Email: wangziying@sdu.edu.cn.
Min Liu, Department of Pharmacology, School of Basic Medical Sciences, Shandong University, Jinan, 250012, China. Tel: 86-531-88382036, Fax: 86-531-88382036, Email: liuweimin@sdu.edu.cn.

Abstract

Background and aims: Podocyte injury is considered as the most important early event contributing to diabetic kidney disease (DKD). Recent findings provide new insights into the roles of lipids and lipid-modulating proteins as key determinants of podocyte function in health and kidney disease. CCDC92, a novel member of coiled-coil domain-containing protein family, was indicated relevant to lipid metabolism, coronary heart disease and type 2 diabetes. However, the expression pattern and role of CCDC92 in the kidney is not clear. This study was designed to elucidate the contribution of CCDC92 in the pathogenesis of DKD.

Methods: Sections with a pathological diagnosis of different classes of DKD, including subjects with mild DKD (class II, n = 6), subjects with moderate DKD (class III, n = 6) or subjects with severe DKD (class IV, n = 6), and control samples (n = 12) were detected for the expression level of CCDC92 and lipid accumulation. Two types of diabetic mice model (*db*/*db* and HFD/STZ) in podocyte-specific *Ccdc92* knockout background were generated to clarify the role of CCDC92 in podocyte lipotoxicity.

Results: The level of CCDC92 was increased in renal biopsies sections from patients with DKD, which was correlated with eGFR and lipid accumulation in glomeruli. In animal studies, CCDC92 were also induced in the kidney from two independent diabetic models, especially in podocytes. Podocyte-specific deletion of *Ccdc92* ameliorated podocyte injury and ectopic lipid deposition under diabetic condition. Mechanically, CCDC92 promoted podocyte lipotoxicity, at least in part through ABCA1 signaling-mediated lipid homeostasis.

Conclusion: Our studies demonstrates that CCDC92 acts as a novel regulator of lipid homeostasis to promote podocyte injury in DKD, suggesting that CCDC92 might be a

potential biomarker of podocyte injury in DKD, and targeting CCDC92 may be an effective innovative therapeutic strategy for patients with DKD.

Keywords: CCDC92; podocytes; lipotoxicity; diabetic kidney disease

Abbreviations

DKD, diabetic kidney disease; DM, diabetes mellitus; ESRD, end-stage renal disease; CCDC, coiled-coil domain-containing; GWAS, genome-wide association studies; UACR, urine albumin to creatinine ratio; Cre, cre recombinase; KO, knock out; ND, normal diet; DAPI, 4',6-diamidino-2-phenylindole; HFD, high-fat diet; STZ, streptozotocin; WT1, Wilms tumor type 1; AAV, adeno-associated virus; WT, wild type; HBSS, Hanks' balanced salt solution; PAS, periodic-acid-schiff; PFA, paraformaldehyde; UPLC, Ultra performance liquid chromatography; MS, mass spectrometry; HPC, human podocyte; MPC, mouse podocytes; GENC, rat glomerular endothelial cells; RMC, rat mesangial cells; NRK-52E, rat proximal tubule epithelial cells; T2D, type 2 diabetes; IF, immunofluorescent; IHC, immunohistochemistry; HG, high glucose; oxLDL, oxidized low-density lipoprotein; GBM, glomerular basement membrane; CD2AP, CD2 associated protein; uPAR, urokinase plasminogen activator receptor; CE, cholesteryl esters; FFA, free fatty acids; TG, triglyceride; PC, phosphatidylcholines; PE, phosphatidylethanolamines; SM, sphingomyelin; SREBP1, sterol-regulatory element binding protein1; SREBP2, sterol-regulatory element binding protein2; ABCA1, ATP-binding cassette transporter A1; ABCG1, ATP-binding cassette transporter G1; PPARα, peroxisome proliferator-activated receptor α; LDLR, low-density lipoprotein receptor; SMPDL3b, sphingomyelin phosphodiesterase acid-like 3b; SNPs, single nucleotide polymorphisms; SD, slit diaphragm; ISGs, interferon-stimulated genes; STRING, Search Tool for the Retrieval of Interacting Genes; IFN-γ, recombinant interferon-γ.

1. Introduction

Diabetic kidney disease (DKD) is one of the major microvascular complications of diabetes mellitus (DM) and the most common cause of end-stage renal disease (ESRD) worldwide, but current therapeutic options for DKD prevention and treatment are limited [1]. Podocytes, the unique terminally differentiated glomerular epithelial cells, are critical for maintaining integrity of glomerular filtration barrier [2]. Podocyte injury is considered as the most important early event contributing to DKD [3]. Although considerable advances have been made in the understanding of mechanisms that trigger podocyte injury, cell-specific and effective treatments are not clinically available [4]. Notably, recent findings provide new insights into the roles of lipids and lipid-modulating proteins as key determinants of podocyte function in health and kidney disease [5]. Moreover, podocytes are more vulnerable to lipid accumulation [6]. Accumulated evidence reported that excessive lipid accumulation in podocytes can lead to lipotoxicity, thereby eventually triggering podocyte hypertrophy, dedifferentiation, mesenchymal transition, derangements of the actin cytoskeleton and death [7]. Therefore, a better understanding of podocyte lipid metabolism will provide unexpected opportunities for developing new therapies for patients with DKD.

The coiled-coil domain-containing (CCDC) proteins have been implicated in a variety of physiological and pathological processes [8]. The unique coiled-coil motif enables the CCDC protein to form a cytoskeleton and regulate cell polarity and movement, molecular recognition and signal transduction as well as other functions [9, 10]. Among CCDC proteins, CCDC92 is a novel member of CCDC family located on chromosome 12q24 which encodes a protein of 331 amino acids in human [11]. Genome-wide association studies (GWAS) indicate that genetic variants of CCDC92 are markedly associated with lipid metabolism [12]. Several independent studies have

shown that CCDC92 is a potential risk gene for coronary heart disease and type 2 diabetes, and the mutation of CCDC92 was closely related to the peripheral fat volume of patients with insulin resistance [13-16]. Notably, a very recent study has demonstrated that *Ccdc92* deletion can reduce obesity, inhibit the inflammatory response in white adipose tissue, and increase systemic insulin sensitivity [17]. However, there is a lack of experimental and clinical evidence to confirm the role of CCDC92 in the kidney although GWAS meta-analysis revealing that genetic variation at the CCDC92 locus is correlated with renal dysfunction [18]. In this study, we found that the level of CCDC92 was increased in renal biopsies from patients with DKD, especially in podocytes, and the upregulation of CCDC92 in glomeruli was correlated with eGFR and lipid accumulation. Podocyte-specific deletion of *Ccdc92* ameliorated podocyte injury and proteinuria in diabetic mice. We further demonstrated a novel role of CCDC92 in modulating ABCA1 signaling-mediated podocyte lipid homeostasis. Our findings indicate that CCDC92 may represent an attractive biomarker as well as a novel therapeutic target for DKD.

2. Materials and methods

Other details for the material and methods are presented in the Supplementary Materials.

2.1. Human renal biopsy samples

Renal biopsies were performed as part of routine clinical diagnostic investigation and collected. Sections of renal biopsies were obtained from Department of Pathology, Shandong University School of Basic Medical Sciences, and Department of Pathology, Shandong Provincial Third Hospital. The control samples were obtained from patients with healthy kidney poles, which underwent tumor nephrectomy and were not diagnosed with diabetes or other kidney diseases. The investigations were

conducted in accordance with the principles of the Declaration of Helsinki and approved by the Research Ethics Committee of Shandong University (Document No. ECSBMSSDU2018-1-021) after informed consent was obtained from the subjects.

A total of 30 renal tissue specimens were collected with the detailed information described in Supplemental Table S1. All the samples of renal biopsies diagnosed as DKD were classified in accordance with a pathologic classification provided by the Renal Pathology Society [19]. From mild to severe, DKD was divided into four hierarchical glomerular lesions as follows: Class I, glomerular basement membrane thickening: isolated glomerular basement membrane thickening and only mild, nonspecific changes by light microscopy that do not meet the criteria of classes II through IV. Class II, mild (IIa) or severe (IIb) mesangial expansion: glomeruli classified as mild or severe mesangial expansion but without nodular sclerosis (Kimmelstiel-Wilson lesions) or global glomerulosclerosis in more than 50% of glomeruli. Class III, nodular sclerosis: at least one glomerulus with nodular increase in mesangial matrix (Kimmelstiel-Wilson) without changes described in class IV. Class IV, advanced diabetic glomerulosclerosis: more than 50% global glomerulosclerosis with other clinical or pathologic evidence that sclerosis is attributable to DKD.

2.2. Animal Studies

All experimental protocols for animal studies were approved by the Institutional Animal Care and Use Committee of School of Basic Medical Sciences, Shandong University (Document No. ECSBMSSDU2018-2-039) and conducted in accordance with the National Institutes of Health Guide for the Care and Use of Laboratory Animals.

2.3. Generation of podocyte-specific *Ccdc92* knockout mice

Ccdc92$^{flox/+}$ (*Ccdc92*$^{fl/+}$) mice (C57BL/6J) were generated by standard homologous recombination at Shanghai Model Organisms Center, Inc. (Shanghai, China), which were crossed with mice expressing Cre recombinase under the control of the podocin promoter (B6. Cg-Tg [*Nphs2-cre*] 295Lbh/J; Jackson Laboratory) to generate podocyte-specific *Ccdc92* knockout (*Podocin-Cre/Ccdc92*$^{fl/fl}$; *Cre*$^{+}$*/Ccdc92*$^{fl/fl}$) mice. Mice with two wild type (WT) alleles and Cre expression were used as controls (*Podocin-Cre/Ccdc92*$^{+/+}$; *Cre*$^{+}$*/Ccdc92*$^{+/+}$). Genotyping by tail preparation and PCR were performed at 2 weeks of age. The primers for genotyping as described in Supplementary Table S2.

2.4. STZ/HFD-induced diabetic mice

We used low-dose STZ-treated uninephrectomized mice on a high-fat diet (HFD) to induce DKD as described in previous studies [7]. Considering the resistance of female mice [20, 21], only male mice were used. Six-week-old male *Cre*$^{+}$*/Ccdc92*$^{fl/fl}$ mice and their littermate were fed either a HFD (60 kcal% from fat, Research Diets, D12492) or control diet (Research Diets, D12450J) for 4 weeks and then uninephrectomized. After a period of recovery, mice were injected low-dose STZ dissolved in 50 mmol/L sodium citrate buffer (pH 4.5) (50mg/Kg/d) intraperitoneally for 3 days after starving for 4 h or vehicle for control. Mice continued to be maintained on a HFD or control diets for another 12 weeks. At the end of the study, blood and 24 h urine samples were collected for biochemical analysis. Simultaneously, the mice were euthanized and the kidney samples were harvested.

2.5. Spontaneous type 2 diabetic *db/db* (BKS) mice

Heterozygote BKS *db/m* mice (BKS.Cg-Dock7^{m} +/+Lepr^{db}/J, Stock No. 000642) and homozygote BKS *db/db* mice (B6. BKS (D)-Lepr^{db}/J, Stock No.000697) were purchased from Jackson Laboratory in the United States. *db/db* mice also could be

obtained by self-crossing of *db/m* mice. *db/db* mice produced identifiable obesity phenotypes at 3-4 weeks of age, with elevated blood glucose at 4-8 weeks. *db/m* mice were used as genetic control. Proteinuria will be observed at age of 8-20 weeks as a marker of successful establishment of type 2 DKD models.

2.6. Generation of podocyte-specific *Ccdc92* knockout mice with spontaneous type 2 diabetes

Podocyte-specific *Ccdc92* knockout mice with spontaneous type 2 diabetes (*db/db//Cre*$^{+}$*/Ccdc92*$^{fl/fl}$) were generated referring to the methods in previous studies [7]. In brief, *db/db//Cre*$^{+}$*/Ccdc92*$^{fl/fl}$ were constructed by crossbreeding *db/+* with *podocin-Cre Ccdc92*$^{fl/fl}$ (*Cre*$^{+}$*/Ccdc92*$^{fl/fl}$, C57BL/6J) mice, followed by mating *db/+//Cre*$^{+}$*/Ccdc92*$^{fl/+}$ with *db/+//Cre*$^{-}$*/Ccdc92*$^{fl/fl}$ or *db/+//Cre*$^{-}$*/Ccdc92*$^{fl/+}$ mice, creating *db/db//Cre*$^{+}$*/Ccdc92*$^{fl/fl}$ and *db/db//Cre*$^{+}$*/Ccdc92*$^{+/+}$ mice. Genotyping by tail preparation and PCR was performed at 2 weeks of age. 24 h urine samples were collected at 4, 8, 12, 16 and 20 weeks old respectively. At the end of 20 weeks, blood and kidney samples were harvested for biochemical testing and histopathological analysis.

2.7. Intrarenal adeno-associated virus delivery

Recombinant adeno-associated virus serotype 9 (AAV9) has been considered as one of the most efficient recombinant AAV serotypes for kidney gene delivery [22]. Meanwhile, we further utilized the recombinant AAV9 vector containing the *Nphs1* promoter to drive expression of *Ccdc92* (*pAV-Nphs1-Ccdc92,* ViGene Biosciences, Shandong, China) or *shRNA* for *Abca1* (*pAV-Nphs1-shAbca1*, ViGene Biosciences, Shandong, China) in podocytes to overcome the non-specificity of recombinant AAV9 [22, 23]. The recombinant AAV9 was delivered into the mouse kidney by means of intraparenchymal injections. The procedure for intrarenal gene delivery was

performed as described with slight modification [24-26]. In anesthetized mice, after temporary occlusion of left renal pedicle, a 31 G needle was inserted at the lower pole of the kidney parallel to the long axis and was carefully pushed toward the upper pole. As the needle was slowly removed, 10-20 μL filter-purified AAV-*Ccdc92*, AAV-*shAbca1* (1×10^{13} IU/μL) or AAV-*NC* was injected. Another 5-10 μL AAV vectors were injected via a second injection route which is parallel but biased towards the lateral border of the kidney. Podocyte-specific AAV 9 harboring *Ccdc92*, *shAbca1* or their negative controls (AAV-*NC*) were delivered into the mouse kidney 4 weeks before STZ injection.

2.8. UPLC–MS/MS analysis

Cell samples from different groups of podocytes were used for lipidomics analysis. Cell pellets containing at least 1×10^6 cells per sample *in vitro* were subjected to liquid extraction. Ultra Performance Liquid Chromatography (UPLC) and tandem mass spectrometry (MS/MS) analysis was performed at Wuhan Metware Biotechnology Co., Ltd (Wuhan, China).

2.9. Cell culture

Conditionally immortalized human and mouse podocyte cell line (HPC, MPC) were provided by Dr Saleem MA from University of Bristol at UK and Prof. Pin-Lan Li from Department of Pharmacology, Virginia Commonwealth University, USA, respectively, and cultured as previous studies [27, 28]. Primary rat glomerular mesangial cells (RMC, CP-R057) and glomerular endothelial cells (GENC, CP-R063) were obtained from Procell Life Science & Technology Co., Ltd. (Wuhan, Hubei, China) and cultured in the specific complete medium (CM-R057 and CM-R063, respectively). Rat proximal tubule epithelial cells (NRK-52E) were obtained from American Type Culture Collection (ATCC) and cultured in DMEM containing FBS

and penicillin/streptomycin.

2.10. Statistics

Data are expressed as mean ± SEM. Statistical analyses were performed with GraphPad Prism (version 8.0, GraphPad Software, San Diego, CA). Details regarding statistics can be found in the Supplementary Materials.

3. Results

3.1. CCDC92 was significantly induced in podocytes under diabetic conditions.

Firstly, we found that CCDC92 was expressed in isolated perfused organs including kidney (Figure 1a) and in various kinds of renal parenchymal cells such as conditionally immortalized human podocyte cell line (HPC), conditionally immortalized mouse podocyte cell line (MPC), rat glomerular endothelial cells (GENC), rat mesangial cells (RMC) and rat proximal tubule epithelial cells (NRK-52E) (Figure 1b) by Western blot analysis. We further assessed the expression patterns of CCDC92 in the whole kidney by immunohistochemistry staining and found Ccdc92 was significantly upregulated in glomeruli but there were no obvious changes in tubules from *db/db* mice (Figure 1c, the detailed information was shown in Supplementary Figure S1a), a spontaneous model of type 2 diabetes (T2D) with phenotype of kidney injury. Meanwhile, Western blotting showed CCDC92 was upregulated in isolated glomeruli from *db/db* mice (20-week age) and streptozotocin plus high fat diet (STZ/HFD)-induced diabetic mice, a late-stage T2D animal model (Figure 1d and e). There was no staining with anti-CCDC92 antibody in the kidney from global *Ccdc92* knockout (*Ccdc92*$^{-/-}$) mice, indicating the specificity of the CCDC92 immunostaining (Supplementary Figure S2a). Moreover, immunofluorescent (IF) results further showed more abundant CCDC92 expression in podocytes from diabetic mice compared to their controls (Figure 1f and g), indicating

that CCDC92 might be involved in podocyte injury in DKD.

In vitro, the expression of CCDC92 was significantly increased in podocytes treated with serum obtained from DKD patients (Figure 1h, Supplementary Table S1). Considering that hyperglycemia and hyperlipidemia are the most prominent risk factors in diabetes, we further exposed podocytes to high glucose (HG) and oxidized low-density lipoprotein (oxLDL), both induced CCDC92 expression (Figure 1i and j). Consistent with *in vivo* studies, there was no obvious changes in CCDC92 expression in NRK-52E treated by high glucose (Figure 1k), indicating that CCDC92 might be involved in podocyte injury under diabetic conditions.

3.2. Upregulation of CCDC92 in renal biopsies from patients with DKD.

A total of 30 renal tissue specimens were collected (the detailed information in Supplementary Table S1), including normal nephrectomy samples adjacent to tumors (n = 12, Scr: 70.6±6.8 μmol/L; eGFR: 105.5±11.8 mL/min/1.73m^2), patients with mild DKD (class II, n = 6, Scr: 113.2±14.2 μmol/L; eGFR: 59.6±13.7 mL/min/1.73m^2), patients with moderate DKD (class III, n = 6, Scr: 134.3±17.5 μmol/L; eGFR: 48.3±10.4 mL/min/1.73m^2) or patients with severe DKD (class IV, n = 6, the Scr: 170.8±48.5 μmol/L; eGFR: 37.9±10.0 mL/min/1.73m^2). By the detection of mRNA levels of CCDC92 in the renal biopsy specimen, we found CCDC92 was significantly induced in the cortex of kidney from DKD patients compared with that of nondiabetic control kidneys (Figure 2a). Moreover, immunohistochemical staining showed that CCDC92 was upregulated in glomeruli, especially in podocytes, from DKD patients than normal subjects (Figure 2b). Interestingly, the expression of CCDC92 was increased in glomeruli from DKD patients with increasing stages. In addition, we further confirmed the upregulation of CCDC92 in podocytes from the renal biopsies with DKD by double immunofluorescence staining (Figure 2c).

Notably, the level of CCDC92 in glomeruli was positively correlated with serum creatinine (Figure 2d), negatively correlated with the estimated GFR (eGFR, Figure 2e) in all subjects.

3.3. Podocyte-specific *Ccdc92* deletion alleviated renal injury in diabetic mice.

To further elucidate the role of CCDC92 in podocytes under diabetic conditions, we generated podocyte-specific *Ccdc92* knockout mice by using *Cre-LoxP* recombination system, which were validated by tail genotyping (Figure 3a), immunofluorescent staining in podocytes (Figure 3b and Supplementary Figure S3a) and Western blot analysis for CCDC92 expression in isolated glomeruli (Figure 3c). All mice were viable and fertile. Mice with podocyte-specific knockout of *Ccdc92* in the *db*/*db* background (*db/db/Cre*$^{+}$*/Ccdc92*$^{fl/fl}$) were generated by crossbreeding *db*/+ with *Cre*$^{+}$*/Ccdc92*$^{fl/fl}$ mice. Then *db/db/Cre*$^{+}$*/Ccdc92*$^{fl/fl}$, *db/db/Cre*$^{+}$*/Ccdc92*$^{+/+}$ and their controls in age matched groups were analyzed in this study. At 20 weeks of age, *db/db* mice had hyperglycemia and higher body weight than those of *db*/+ mice (Supplementary Table S3). In a 20-week follow-up, *db/db/Cre*$^{+}$*/Ccdc92*$^{+/+}$ mice developed albuminuria as evidenced by the higher levels of urine albumin to creatinine ratio (UACR), which were much lower in *db/db/Cre*$^{+}$*/Ccdc92*$^{fl/fl}$ mice (Figure 3d). Morphological examinations showed glomerular and podocyte injuries in *db/db/Cre*$^{+}$*/Ccdc92*$^{+/+}$ mice as evidenced by glomerular basement membrane (GBM) thickening, podocyte foot process broadening and effacement, all of which were alleviated in *db/db/Cre*$^{+}$*/Ccdc92*$^{fl/fl}$ group (Figure 3e). Furthermore, *Ccdc92* deletion recovered the expression of key podocyte differentiation markers including nephrin, podocin, synaptopodin, and CD2 associated protein (CD2AP) in isolated glomeruli of diabetic mice (Figure 3f). In addition, considering that urokinase plasminogen activator receptor (uPAR) is regarded as a key factor for podocyte foot process

effacement and proteinuria, we further detected the uPAR expression in different groups of mice and found *db/db/Cre*$^{+}$*/Ccdc92*$^{+/+}$ mice had a significant increase in podocyte uPAR expression, which was attenuated by *Ccdc92* deletion (Figure 3g). The protective role of CCDC92 deficiency in podocyte was further confirmed in STZ/HFD induced diabetic mice (Supplementary Figure S4, Supplementary Table S3).

3.4. CCDC92 contributed to podocyte lipotoxicity under diabetic conditions.

Notably, *db/db/Cre*$^{+}$*/Ccdc92*$^{fl/fl}$ mice had fewer neutral lipids deposition in glomeruli by Oil Red O staining (Figure 4a), as well as lower lipid droplets in podocytes assessed by adipophilin staining, a lipid droplet-specific marker, compared with *db/db/Cre*$^{+}$*/Ccdc92*$^{+/+}$ mice (Figure 4b). Meanwhile, we also demonstrated that gene silencing of *Ccdc92* (Supplementary Figure S5a) decreased the accumulation of lipid in conditionally immortalized human podocyte cell line (HPC) with HG treatment (Figure 4c and d). By LC/MS-based lipidomics analysis, we found that gene ablation of *Ccdc92* significantly reduced the levels of cholesteryl esters (CE, Figure 4e), free fatty acids (FFA, Figure 4f) and triglyceride (TG, Figure 4g) in HPC with HG treatment, with a reduced tendency of some other lipids, such as phosphatidylcholines (PC, Supplementary Figure S5b), ceramides (Supplementary Figure S5c), phosphatidylethanolamines (PE, Supplementary Figure S5d) and sphingomyelin (SM, Supplementary Figure S5e). Moreover, gene silencing of *Ccdc92* reverted the expression of nephrin and podocin (Figure 4h and i), attenuated cell apoptosis (Figure 4j) and reduced the levels of proinflammatory mediators (Figure 4k) in HPC with high glucose treatment.

To further examine the role of CCDC92, STZ/HFD-induced DKD mice were transfected by a podocyte-specific AAV serotype 9 harboring Ccdc92

(*pAV-Nphs1-Ccdc92*) through intraparenchymal injections. The efficiency of gene transfection in glomeruli and podocytes was confirmed by Western blot and IF analyses (Figure5a and b, Supplementary Figure S6a). There were no significant changes of urinary albumin excretion or glomerular mesangial expansion in AAV-*Ccdc92* mice under normal conditions (Figure 5c and d). However, overexpression of *Ccdc92* in podocytes increased albuminuria, mesangial expansion, foot process fusion and detachment (Figure 5c-e) as well as lipid accumulation (Figure 5f and g) in glomeruli, especially in podocytes, suggesting *Ccdc92* exacerbated podocyte lipotoxicity injury in diabetic mice.

3.5. *Ccdc92* deficiency reduced intracellular lipid accumulation by the upregulation of ABCA1 in podocytes under diabetic conditions.

Based on lipidomic analysis that CCDC92 was involved in lipid metabolism in podocytes under diabetic conditions, we then evaluated the levels of some key molecules in the regulation of lipid homeostasis, such as sterol-regulatory element binding protein1 (SREBP1), SREBP2, ATP-binding cassette transporter A1 (ABCA1), ABCG1, peroxisome proliferator-activated receptor α (PPARα), low-density lipoprotein receptor (LDLR), and sphingomyelin phosphodiesterase acid-like 3b (SMPDL3b). Although all of them were changed under HG condition, gene silencing of *Ccdc92* preferentially reversed the expression of ABCA1 (Figure 6a). We further confirmed that *Ccdc92* deficiency enhanced the protein level of ABCA1 in glomeruli and podocytes from diabetic mice (Figure 6b and c). Notably, our results showed that the expression of ABCA1 was significantly downregulated in glomeruli from patients with DKD, with accumulation of lipid and podocyte loss evidenced by adipophilin and WT1 staining, respectively (Figure 6d). Importantly, the expression of ABCA1 in glomeruli was negatively correlated with lipid accumulation and podocyte loss

(Figure 6e and f), suggesting that ABCA1 was involved in podocyte lipotoxicity. However, the level of CCDC92 was negatively correlated with ABCA1 (Figure 6g) while positively correlated with the degree of lipid accumulation (Figure 6h) in glomeruli from patients with DKD, indicating that ABCA1 might be involved in the CCDC92-mediated podocyte lipotoxicity injury.

To further investigate whether ABCA1 is a key regulator linking CCDC92 and podocyte injury in DKD, a podocyte-specific AAV serotype 9 harboring *shAbca1* (*pAV-Nphs1-shAbca1*) was delivered into *podocin-Cre Ccdc92*$^{fl/fl}$ mice by means of intraparenchymal injections (Figure 7a, Supplementary Figure S7a). Our results showed that although conditional knockout of *Ccdc92* attenuated GBM and podocyte injury under diabetic condition, knockdown of *Abca1* in podocytes counteracted the effects of *Ccdc92* deletion as evidenced by increased level of proteinuria and glomerular expansion, decreased expression levels of nephrin and podocin (Figure 7b-d). Importantly, we further demonstrated that gene silencing of *Abca1* upregulated ectopic lipid deposition in glomeruli and conditionally immortalized human podocytes (Figure 7e and f), abolishing the protective role of *Ccdc92* deficiency under diabetic condition.

4. Discussion

Although recent studies have indicated that CCDC92 is involved in the metabolic diseases, whether CCDC92 is expressed in the kidney and its related biological functions remain unclear [18], [29]. In this study, we found for the first time that CCDC92 was expressed in different types of renal parenchymal cells and the level of CCDC92 was significantly increased in glomeruli from DKD patients with increasing stages and positively correlated with serum creatinine but negatively correlated with the estimated GFR, indicating that CCDC92 expression correlated with the severity of

DKD. In particular, we also identified that CCDC92 was upregulated in podocytes from DKD. Considering that podocyte injury is considered as the most important early event contributing to DKD and loss of podocytes is an independent predictor of DKD progression [2], our results suggest that CCDC92 might be a potential biomarker for DKD and predict the progression of kidney damage.

As evidence continues to accumulate demonstrating the link between disturbances of podocyte lipid metabolism and kidney disease, such insight will open up potential new therapeutic avenues for patients with diabetic and other proteinuric nephropathy [30, 31]. Among different types of renal parenchymal cells, podocytes are particularly susceptible to lipid accumulation. Moreover, dysregulation of intracellular lipid homeostasis will result in cellular dysfunction and eventually trigger cell death, which is regarded as podocyte lipotoxicity [32, 33]. Our previous studies have demonstrated that excessive lipid accumulation exacerbates podocyte injury in DKD [7]. Additionally, recent studies have reported that the CCDC92 is related to the type 2 diabetes and coronary heart disease [12-14], and knockdown of *Ccdc92* significantly reduces lipid accumulation in a mouse adipocyte model [15], suggesting that *Ccdc92* may be involved in lipid metabolism. Here, we further found that *Ccdc92* deficiency markedly reduced ectopic lipid deposition in glomeruli, especially in podocytes, thereby leading to reducing proteinuria, glomerular expansion and podocyte injury. Consistently, gene silence of *Ccdc92* inhibited cell apoptosis, inflammatory response as well as diminution of slit diaphragm (SD) proteins in podocytes with HG treatment, all of them are regarded as features of podocyte lipotoxicity [5, 34], suggesting CCDC92 contributes to podocyte lipotoxicity injury in DKD. Moreover, we further demonstrated that *Ccdc92* overexpression in podocytes significantly exacerbated kidney injury and podocyte lipotoxicity under diabetic condition, further indicating

that CCDC92 might be an attractive target of novel therapeutic strategies for DKD and other podocytopathies.

It is known that pathologic lipid deposition in podocytes is a consequence of the dysregulation of genes or proteins involved in cellular lipid metabolism, which comprises synthesis, uptake, storage, utilization, and cellular efflux rather than the amount of circulating lipids [7, 31, 35]. Therefore, we further evaluated the levels of some key molecules which are involved in the regulation of cellular lipid homeostasis [36]. Among them, *Ccdc92* deficiency markedly restored the decreased level of ABCA1 in podocytes under diabetic conditions. ABCA1 is a transmembrane protein that regulates the translocation of sterol and phospholipids [37]. Studies have reported that the level of ABCA1 is inversely correlated with serum creatinine in patients with DKD. Moreover，*Abca1* deficiency is a susceptibility factor in podocyte injury and podocyte-specific deletion of *Abca1* aggravates kidney injury in mice with DKD [38]. Importantly, ABCA1 serves as a master switch to maintain lipid homeostasis by mediating intracellular lipid outflow, suggesting the important role of ABCA1 in lipid metabolism and podocyte injury in DKD [38-40]. In this study, we found the expression of ABCA1 was significantly reduced in glomeruli from patients with DKD and the expression of ABCA1 in glomeruli was negatively correlated with CCDC92, lipid accumulation and podocyte loss. In particular, ABCA1 knockdown counteracted the protective effects of *Ccdc92* deficiency in podocytes. Collectively, our results indicate that ABCA1 might be one of the critical components that links CCDC92 to podocyte lipotoxicity in the pathogenesis of diabetic nephropathy.

It should be noted that there are some limitations in this study. First, although we have revealed a novel role of CCDC92 in regulating podocyte lipid metabolism through ABCA1, we cannot exclude that other regulators may also be involved in this process.

Second, we did not delineate the mechanisms by which induce CCDC92 expression under diabetic conditions. However, previous studies suggested that CCDC92 is one of the interferon-stimulated genes (ISGs), which can be induced by the activation of JAK/STAT pathways [41]. Therefore, it is necessary to further clarify the role of JAK/STAT signaling as well as other potential regulators on the regulation of CCDC92. In addition, the molecular mechanism by which CCDC92 regulated ABCA1 is also needed to be elucidated. The prediction by Search Tool for the Retrieval of Interacting Genes (STRING) indicates CCDC92 may interact with various units of protease, we are exploring the mechanism by which CCDC92 could regulate the degradation of ABCA1 by ubiquitin proteasome system, ongoing studies will address this issue.

5. Conclusion

Collectively, our studies for the first time demonstrate that CCDC92 acts as a novel regulator of lipid homeostasis to promote podocyte and glomerular injuries, at least in part through regulation of ABCA1. CCDC92 is expected to become a potential biomarker of podocyte injury in DKD, genetic or pharmacological targeting of CCDC92 may provide a novel approach for the treatment of DKD and other glomerular diseases.

CRediT authorship contribution statement

Fuwen Zuo conducted *in vivo* and *in vitro* experiments, performed data analysis, and helped write the manuscript. Youzhao Wang and Xiaojie Wang performed *in vivo* animal studies. Xinlei Xu and Ruihao Ding performed *in vitro* experiments. Wei Tang and Yu Sun analyzed the data. Yan Zhang and Yusheng Xie helped design experiments. Jichao Wu performed the confocal microscopy. Fan Yi, Ziying Wang

and Min Liu designed the experiment, interpreted the data, wrote the manuscript, and approved final version of the manuscript for publication.

Declaration of competing interest

All the authors declared no competing interests.

Data availability

All the data that support the findings of this study are available from the corresponding author upon reasonable request.

Acknowledgements

This study was supported by The National Nature Science Foundation of China (91949202, 82090024, 81873614, 82090021, 81900621, 81970580, 82070753, 82170734, T2321004, 81800645, 81800643); Shandong Provincial Natural Science Foundation, China (ZR2019ZD40, ZR2019MH041).

References

[1] Lytvyn Y, Bjornstad P, van Raalte DH, Heerspink HL, Cherney DZI. The New Biology of Diabetic Kidney Disease-Mechanisms and Therapeutic Implications. Endocr Rev. 2020;41.

[2] Torban E, Braun F, Wanner N, Takano T, Goodyer PR, Lennon R, et al. From podocyte biology to novel cures for glomerular disease. Kidney Int. 2019;96:850-61.

[3] Reidy K, Kang HM, Hostetter T, Susztak K. Molecular mechanisms of diabetic kidney disease. J Clin Invest. 2014;124:2333-40.

[4] Nagata M. Podocyte injury and its consequences. Kidney Int. 2016;89:1221-30.

[5] Sun Y, Cui S, Hou Y, Yi F. The Updates of Podocyte Lipid Metabolism in Proteinuric Kidney Disease. Kidney Dis (Basel). 2021;7:438-51.

[6] Meyer-Schwesinger C. The ins-and-outs of podocyte lipid metabolism. Kidney Int. 2020;98:1087-90.

[7] Fu Y, Sun Y, Wang M, Hou Y, Huang W, Zhou D, et al. Elevation of JAML Promotes Diabetic Kidney Disease by Modulating Podocyte Lipid Metabolism. Cell Metab. 2020;32:1052-62 e8.

[8] Burkhard P, Stetefeld J, Strelkov SV. Coiled coils: a highly versatile protein folding motif. Trends Cell Biol. 2001;11:82-8.

[9] Apostolovic B, Danial M, Klok HA. Coiled coils: attractive protein folding motifs for the fabrication of self-assembled, responsive and bioactive materials. Chem Soc Rev. 2010;39:3541-75.

[10] Truebestein L, Leonard TA. Coiled-coils: The long and short of it. Bioessays. 2016;38:903-16.

[11] Chasman DI, Pare G, Mora S, Hopewell JC, Peloso G, Clarke R, et al. Forty-three loci associated with plasma lipoprotein size, concentration, and cholesterol content in genome-wide analysis. PLoS Genet. 2009;5:e1000730.

[12] Ross S, Gerstein H, Pare G. The Genetic Link Between Diabetes and Atherosclerosis. Can J Cardiol. 2018;34:565-74.

[13] Zhao W, Rasheed A, Tikkanen E, Lee JJ, Butterworth AS, Howson JMM, et al. Identification of new susceptibility loci for type 2 diabetes and shared etiological pathways with coronary heart disease. Nat Genet. 2017;49:1450-7.

[14] Klarin D, Zhu QM, Emdin CA, Chaffin M, Horner S, McMillan BJ, et al. Genetic analysis in UK Biobank links insulin resistance and transendothelial migration pathways to coronary artery disease. Nat Genet. 2017;49:1392-7.

[15] Lotta LA, Gulati P, Day FR, Payne F, Ongen H, van de Bunt M, et al. Integrative genomic analysis implicates limited peripheral adipose storage capacity in the pathogenesis of human insulin resistance. Nat Genet. 2017;49:17-26.

[16] Xiao L, Shi D, Zhang H, Zhang Y, Liu Y, Lu H, et al. Association between single nucleotide polymorphism rs11057401 of CCDC92 gene and the risk of coronary heart disease (CHD). Lipids Health Dis. 2018;17:28.

[17] Ren L, Du W, Song D, Lu H, Hamblin MH, Wang C, et al. Genetic ablation of diabetes-associated gene Ccdc92 reduces obesity and insulin resistance in mice. iScience. 2023;26:105769.

[18] Shungin D, Winkler TW, Croteau-Chonka DC, Ferreira T, Locke AE, Magi R, et al. New genetic loci link adipose and insulin biology to body fat distribution. Nature.

2015;518:187-96.

[19] Tervaert TWC, Mooyaart AL, Amann K, Cohen AH, Cook HT, Drachenberg CB, et al. Pathologic classification of diabetic nephropathy. Journal of the American Society of Nephrology : JASN. 2010;21:556-63.

[20] Prossnitz ER, Barton M. The G protein-coupled oestrogen receptor GPER in health and disease: an update. Nat Rev Endocrinol. 2023;19:407-24.

[21] Le May C, Chu K, Hu M, Ortega CS, Simpson ER, Korach KS, et al. Estrogens protect pancreatic beta-cells from apoptosis and prevent insulin-deficient diabetes mellitus in mice. Proc Natl Acad Sci U S A. 2006;103:9232-7.

[22] Sun H, Li H, Yan J, Wang X, Xu M, Wang M, et al. Loss of CLDN5 in podocytes deregulates WIF1 to activate WNT signaling and contributes to kidney disease. Nature Communications. 2022;13:1600.

[23] Picconi JL, Muff-Luett MA, Wu D, Bunchman E, Schaefer F, Dunphy PD. Kidney-specific expression of GFP by in-utero delivery of pseudotyped adeno-associated virus 9. Molecular Therapy - Methods & Clinical Development. 2014;1.

[24] Kim M, Chen SWC, Park SW, Kim M, D'Agati VD, Yang J, et al. Kidney-specific reconstitution of the A1 adenosine receptor in A1 adenosine receptor knockout mice reduces renal ischemia-reperfusion injury. Kidney International. 2009;75:809-23.

[25] Zhan P, Zhang Y, Shi W, Liu X, Qiao Z, Wang Z, et al. Myeloid-derived growth factor deficiency exacerbates mitotic catastrophe of podocytes in glomerular disease. Kidney International. 2022;102:546-59.

[26] Li Y, Yan H, Wang F, Huang S, Zhang Y, Wang Z, et al. Activation of EphA1-Epha receptor axis attenuates diabetic nephropathy in mice. Biochem Biophys Res Commun. 2017;486:693-9.

[27] Saleem MA, O'Hare MJ, Reiser J, Coward RJ, Inward CD, Farren T, et al. A conditionally immortalized human podocyte cell line demonstrating nephrin and podocin expression. Journal of the American Society of Nephrology : JASN. 2002;13:630-8.

[28] Zhang C, Hu J-J, Xia M, Boini KM, Brimson CA, Laperle LA, et al. Protection of podocytes from hyperhomocysteinemia-induced injury by deletion of the gp91phox gene. Free Radic Biol Med. 2010;48:110.-17.

[29] Priyanka PP, Yenugu S. Coiled-Coil Domain-Containing (CCDC) Proteins: Functional Roles in General and Male Reproductive Physiology. Reprod Sci. 2021;28:2725-34.

[30] de Vries APJ, Ruggenenti P, Ruan XZ, Praga M, Cruzado JM, Bajema IM, et al. Fatty kidney: emerging role of ectopic lipid in obesity-related renal disease. Lancet Diabetes Endocrinol. 2014;2:417-26.

[31] Fornoni A, Merscher S, Kopp JB. Lipid biology of the podocyte--new perspectives offer new opportunities. Nat Rev Nephrol. 2014;10:379-88.

[32] Unger RH, Clark GO, Scherer PE, Orci L. Lipid homeostasis, lipotoxicity and the metabolic syndrome. Biochim Biophys Acta. 2010;1801:209-14.

[33] Nishi H, Nangaku M. Podocyte lipotoxicity in diabetic kidney disease. Kidney International. 2019;96:809-12.

[34] Brinkkoetter PT, Bork T, Salou S, Liang W, Mizi A, Ozel C, et al. Anaerobic Glycolysis Maintains the Glomerular Filtration Barrier Independent of Mitochondrial Metabolism and Dynamics. Cell Rep. 2019;27:1551-66 e5.

[35] D'Agati VD, Chagnac A, de Vries AP, Levi M, Porrini E, Herman-Edelstein M, et al. Obesity-related glomerulopathy: clinical and pathologic characteristics and pathogenesis. Nat Rev Nephrol. 2016;12:453-71.

[36] Yoon H, Shaw JL, Haigis MC, Greka A. Lipid metabolism in sickness and in health: Emerging regulators of lipotoxicity. Mol Cell. 2021;81:3708-30.

[37] Plummer AM, Culbertson AT, Liao M. The ABCs of Sterol Transport. Annu Rev Physiol. 2021;83:153-81.

[38] Ducasa GM, Mitrofanova A, Mallela SK, Liu X, Molina J, Sloan A, et al. ATP-binding cassette A1 deficiency causes cardiolipin-driven mitochondrial dysfunction in podocytes. J Clin Invest. 2019;129:3387-400.

[39] Luo J, Yang H, Song BL. Mechanisms and regulation of cholesterol homeostasis. Nat Rev Mol Cell Biol. 2020;21:225-45.

[40] Wahl P, Ducasa GM, Fornoni A. Systemic and renal lipids in kidney disease development and progression. Am J Physiol Renal Physiol. 2016;310:F433-45

[41] Kuroda M, Halfmann PJ, Hill-Batorski L, Ozawa M, Lopes TJS, Neumann G, et al. Identification of interferon-stimulated genes that attenuate Ebola virus infection. Nat Commun. 2020;11:2953.

Figure legends

Figure 1. CCDC92 was significantly induced in podocytes from different models under diabetic conditions. a. Representative Western blot gel documents and summarized data showing the relative protein levels of CCDC92 in selected mouse tissues including brain, heart, liver, spleen, lung, kidney, fat, testis, stomach and intestines (n = 6 for each group). **b.** Representative Western blot gel documents and summarized data showing the relative protein levels of CCDC92 in renal cells including conditionally immortalized human podocyte cell line (HPC), mouse podocyte cell line (MPC), rat glomerular endothelial cells (GENC), rat mesangial cells (RMC) and rat proximal tubule epithelial cells (NRK-52E) (n = 6 for each group). **c.** Representative IHC images of CCDC92 in glomeruli from different groups of mice. **d.** Isolated glomeruli visualized by light microscopy. **e.** Representative Western blot gel documents and summarized data showing the relative protein levels of CCDC92 in isolated glomeruli from diabetic mice (n = 8 for each group). ***P < 0.001 vs. control. **f.** Representative immunofluorescence images of CCDC92 (green) and synaptopodin (red) in glomeruli from diabetic mice. DAPI (4',6-diamidino-2-phenylindole) was used as a nuclear staining. Arrows indicate representative podocytes. **g.** Representative immunofluorescence images of CCDC92 (green) and synaptopodin (red) in glomeruli from STZ/HFD induced diabetic mice. DAPI was used as a nuclear staining. Arrows indicate representative podocytes. **h.** Representative Western blot gel documents and summarized data showing the relative protein levels of CCDC92 in HPC treated with serum from healthy persons (Healthy) and patients with diabetic kidney disease (DKD) for 24 h (n = 6 for each group). ***P < 0.001 vs. healthy control. **i.** Representative Western blot gel documents and summarized data showing the relative protein levels of CCDC92 in HPC treated with

high glucose (HG, 15 or 30 mmol/L) for 24 h (n = 6 for each group). ***P < 0.001 vs. control. **j.** Representative Western blot gel documents and summarized data showing the relative protein levels of CCDC92 in HPC treated with oxidized low-density lipoprotein (oxLDL, 10-40 μg/mL) for 24 h (n = 6 for each group). **P < 0.01, ***P < 0.001 vs. control. **k.** Representative Western blot gel documents and summarized data showing the relative protein levels of CCDC92 in NRK-52E treated with high glucose (HG, 15 or 30 mmol/L) for 24 h (n = 6 for each group). Data are expressed as mean ± SEM and n indicates the number of biologically independent experiments. Two-tailed Student's unpaired t test analysis (c, e, h), one-way ANOVA followed by Tukey's post-test (i-k).

Figure 2. Upregulation of CCDC92 in renal biopsies from patients with DKD. a. Relative mRNA levels of CCDC92 in human renal cortical tissues from normal subjects (n = 9), subjects with mild (class II, n = 6), moderate (class III, n = 6) or severe (class IV, n = 6) histopathological lesions of DKD. *P < 0.05, **P < 0.01, ***P < 0.001 vs. normal subjects. **b.** Representative immunohistochemistry images and quantification of glomerular CCDC92 expression in human renal cortical tissues from normal subjects (n = 12), subjects with mild (class II, n = 6), moderate (class III, n = 6) or severe (class IV, n = 6) histopathological lesions of DKD. **P < 0.01, ***P < 0.001 vs. normal subjects. **c.** Representative immunofluorescence images and quantification of glomerular CCDC92 expression or Wilms' Tumer 1 (WT-1, used as a podocyte marker) staining in human renal cortical tissues from normal subjects (n = 12) and patients with DKD (n = 18). DAPI (4',6-diamidino-2-phenylindole) was used as a nuclear staining. ***P < 0.001 vs. normal subjects. **d**. Correlation between glomerular CCDC92 expression and SCr in all subjects (n = 18). **e.** Correlation between glomerular CCDC92 expression and eGFR in all subjects (n = 18). Data are

expressed as mean ± SEM and n indicates the number of biologically independent experiments. Kruskal-Wallis test followed by Dunn's post-test (c), one-way ANOVA followed by Tukey's post-test (a-b), Spearman's correlations (d-e).

Figure 3. Podocyte-specific *Ccdc92* deletion alleviated renal injury in diabetic mice. a. Generation of conditional knockout mice in which *Ccdc92* is specifically ablated in podocytes by using *Cre–LoxP* recombination system. Exon 4 is deleted upon *Nphs2-Cre* mediated recombination. Genotyping was confirmed by tail preparation and PCR at 2 weeks of age. **b.** Representative immunofluorescence images of CCDC92 (green) and synaptopodin (red) in glomeruli from $Cre^{+}/Ccdc92^{fl/fl}$ mice, confirming podocyte-specific loss of *Ccdc92* in podocytes in $Cre^{+}/Ccdc92^{fl/fl}$ mice. DAPI (4',6-diamidino-2-phenylindole) was used as a nuclear staining. Arrows indicate representative podocytes. The distribution of CCDC92 gene expression in podocyte-specific *Ccdc92* knockout mice was displayed by the number of glomeruli based on the relative fluorescence intensity (normalized to the average level of controls). 15 glomeruli randomly chosen from each mouse were evaluated in a blinded manner. Dot with different color represents different mouse (n = 6). **c.** Representative Western blot and quantifications of CCDC92 expression in glomeruli from $Cre^{+}/Ccdc92^{+/+}$ and $Cre^{+}/Ccdc92^{fl/fl}$ mice (n = 6 for each group). $^{***}P < 0.001$ vs. $Cre^{+}/Ccdc92^{+/+}$ mice. **d.** Urinary albumin creatinine ratio in different groups of mice at different ages (n = 8 for each group). $^{*}P < 0.05$, $^{***}P < 0.001$ vs. *db/+//*$Cre^{+}/Ccdc92^{+/+}$ mice, $^{\#\#}P < 0.01$, $^{\#\#\#}P < 0.001$ vs. *db/db//*$Cre^{+}/Ccdc92^{+/+}$mice. **e.** Morphological examinations of glomerular changes by Periodic acid–Schiff (PAS) and transmission electron microscopy (TEM) analysis in mice (n = 8 for each group). $^{*}P < 0.05$, $^{**}P < 0.01$, $^{***}P < 0.001$ vs. *db/+//*$Cre^{+}/Ccdc92^{+/+}$ mice, $^{\#\#}P < 0.01$, $^{\#\#\#}P < 0.001$ vs. *db/db//*$Cre^{+}/Ccdc92^{+/+}$mice. **f.** Representative Western blot gel documents

and summarized data showing the relative protein levels of nephrin, podocin, synaptopodin and CD2-associated proteins (CD2AP) in isolated glomeruli from different groups of mice (n = 6 for each group). $^{**}P < 0.01$, $^{***}P < 0.001$ vs. *db/+//Cre*$^{+}$*/Ccdc92*$^{+/+}$ mice, $^{\#\#\#}P < 0.001$ vs. *db/db//Cre*$^{+}$*/Ccdc92*$^{+/+}$ mice. **g.** Representative immunofluorescence images showing the expressions of urokinase type plasminogen activator receptor (uPAR) in podocytes from different groups of mice. DAPI (4', 6-diamidino-2-phenylindole) was used as a nuclear staining. Data are expressed as mean ± SEM and n indicates the number of biologically independent experiments. Two-tailed Student's unpaired t test analysis (c). Two-way ANOVA followed by Tukey's post-test (d-f).

Figure 4. CCDC92 contributed to podocyte lipotoxicity under diabetic conditions.

a. Representative images and quantifications showing lipid deposition by Oil Red O staining in kidney from mice (n = 8 for each group). $^{***}P < 0.001$ vs. *db/+//Cre*$^{+}$*/Ccdc92*$^{+/+}$mice, $^{\#\#\#}P < 0.001$ vs. *db/db//Cre*$^{+}$*/Ccdc92*$^{+/+}$ mice. **b.** Representative images and quantifications showing lipid deposition by immunofluorescence staining of adipophilin (green) and synaptopodin (red) in kidney from mice (n = 8 for each group). DAPI (4',6-diamidino-2-phenylindole) was used as a nuclear staining. $^{**}P < 0.01$, $^{***}P < 0.001$ vs. *db/+//Cre*$^{+}$*/Ccdc92*$^{+/+}$ mice, $^{\#\#\#}P < 0.001$ vs. *db/db//Cre*$^{+}$*/Ccdc92*$^{+/+}$ mice. **c.** Representative Oil Red O images of conditionally immortalized human podocyte cell line (HPC) in different groups. **d.** Representative Nile red staining images of HPC with different groups. DAPI was used as a nuclear staining. **e.** UPLC-MS/MS analysis of HPC with different groups. Ion chromatograms and quantifications of total lipid content by analysis of AUC of cholesteryl esters (CE) in podocytes (n = 6 for each group). $^{***}P < 0.001$ vs. negative

control for *Ccdc92* knockdown (*si-NC*), $^{###}P < 0.001$ vs. negative control of HG treatment. **f.** Total free fatty acids (FFA) content in HPC (n = 6 for each group). $^{**}P < 0.01$, $^{***}P < 0.001$ vs. *si-NC*, $^{\#}P < 0.05$ vs. negative control of HG treatment. **g.** Total triglyceride (TG) content in HPC (n = 6 for each group). $^{**}P < 0.01$, $^{***}P < 0.001$ vs. *si-NC*, $^{\#\#}P < 0.01$ vs. negative control of HG treatment. **h.** Representative Western blot gel documents and summarized data showing the relative protein levels of nephrin in HPC with different treatments (n = 6 for each group). $^{***}P < 0.001$ vs. *si-NC*, $^{###}P < 0.001$ vs. negative control of HG treatment. **i.** Representative Western blot gel documents and summarized data showing the relative protein levels of podocin in HPC with different treatments (n = 6 for each group). $^{*}P < 0.05$, $^{***}P < 0.001$ vs. *si-NC*, $^{###}P < 0.001$ vs. negative control of HG treatment. **j.** Flow cytometry analysis to evaluate the role of CCDC92 on the regulation of apoptosis HPC (n = 6 for each group). $^{***}P < 0.001$ vs. *si-NC*, $^{###}P < 0.001$ vs. negative control of HG treatment. **k.** The levels of pro-inflammatory mediators in HPC with different treatments (n = 6 for each group). Levels of the housekeeping gene β-actin were used as an internal control for the normalization of RNA quantity among the samples. $^{**}P < 0.01$, $^{***}P < 0.001$ vs. *si-NC*, $^{\#\#}P < 0.01$, $^{###}P < 0.001$ vs. negative control of HG treatment. Data are expressed as mean ± SEM and n indicates the number of biologically independent experiments. Two-way ANOVA followed by Tukey's post-test (a-b, e-k).

Figure 5. Overexpression of *Ccdc92* exacerbated podocyte injury in diabetic mice.

a. Representative Western blot gel documents and summarized data showing the transfection efficiency in isolated glomeruli from mice with AAV harboring negative control (AAV-*NC*) or *Ccdc92* (AAV-*Ccdc92)* at 5-week after injection. (n = 8 for

each group). ***P < 0.001 vs. AAV-*NC* mice. **b.** Representative immunofluorescence images of CCDC92 (green) and synaptopodin (red) in glomeruli. DAPI (4',6-diamidino-2-phenylindole) was used as a nuclear staining. Arrows indicate representative podocytes. The distribution of CCDC92 gene expression in AAV harboring *Ccdc92* (AAV-*Ccdc92*) overexpression mice was displayed by the number of glomeruli based on the relative fluorescence intensity (normalized to the average level of controls). 15 glomeruli randomly chosen from each mouse were evaluated in a blinded manner. Dot with different color represents different mouse (n = 6). **c.** Urinary albumin creatinine ratio in different groups of mice (n = 6 for each group). ***P < 0.001 vs. *AAV-NC* mice, $^{###}P$ < 0.001 vs. AAV-*NC* with streptozocin plus high fat diet (STZ/HFD) mice. **d.** Morphological examinations of glomerular changes by Periodic acid–Schiff (PAS) analyses in mice (n = 6 for each group). ***P < 0.001 vs. AAV-*NC* mice, $^{##}P$ < 0.01 vs. AAV-*NC* with STZ/HFD mice. **e.** Morphological examinations of glomerular changes by transmission electron microscopy (TEM) analysis in mice (n = 6 for each group). ***P < 0.001 vs. AAV-*NC* mice, $^{#}P$ < 0.01, $^{##}P$ < 0.001 vs. AAV-*NC* with STZ/HFD mice. **f.** Representative Oil Red O images of podocytes in different groups (n = 6 for each group). ***P < 0.001 vs. AAV-*NC* mice, $^{###}P$ < 0.001 vs. AAV-*NC* STZ/HFD mice. **g.** Representative images and quantifications showing lipid deposition by immunofluorescence staining of adipophilin (green) and synaptopodin (red) in kidney from mice (n = 6 for each group). DAPI was used as a nuclear staining. ***P < 0.001 vs. AAV-*NC* mice, $^{###}P$ < 0.001 vs. AAV-*NC* STZ/HFD mice. Data are expressed as mean ± SEM and n indicates the number of biologically independent experiments. Two-tailed Student's unpaired t test analysis (a), Two-way ANOVA followed by Tukey's post-test (c-g).

Figure 6. *Ccdc92* deficiency reduced intracellular lipid accumulation by

upregulating ABCA1 protein level in podocytes under diabetic conditions.

a. Representative Western blot gel documents and summarized data showing the relative protein levels of some key molecules related to lipid homeostasis in conditionally immortalized human podocyte cell line (HPC) with different treatments (n = 6 for each group). $^{**}P < 0.01$, $^{***}P < 0.001$ vs. negative control for *Ccdc92* knockdown (*si-NC*), $^{\#}P < 0.05$, $^{\#\#\#}P < 0.001$ vs. negative control of HG treatment. **b.** Representative IHC images of ABCA1 in glomeruli from different groups of mice. **c.** Representative IF images of ABCA1 (green) and synaptopodin (red) in glomeruli from different groups of mice. DAPI (4',6-diamidino-2-phenylindole) was used as a nuclear staining. **d.** Photomicrographs and quantifications showing the expression of ABCA1, Adipophilin or Wilms Tumor-1 (WT-1) protein staining in human renal cortical tissue from normal subjects (n = 12) and patients with diabetic kidney disease (DKD, n = 18). WT-1 was used as a marker for podocyte. **e.** Correlation between glomerular expression of ABCA1 and Adipophilin in all subjects (n = 18). **f.** Correlation between glomerular ABCA1 expression and WT-1 in all subjects. (n = 18). **g.** Correlation between glomerular expression of CCDC92 and ABCA1 in all subjects (n = 18). **h.** Correlation between glomerular expression of CCDC92 and Adipophilin in all subjects (n = 18). Data are expressed as mean ± SEM and n indicates the number of biologically independent experiments. Two-way ANOVA followed by Tukey's post-test (a), Kruskal-Wallis test followed by Dunn's post-test (d), Spearman's correlations (e-h).

Figure 7. Podocyte *Abca1* knockdown counteracted the protective effects of *Ccdc92* deletion on podocyte lipotoxicity in DKD mice.

a. Representative Western blot gel documents and summarized data showing the transfection efficiency in isolated glomeruli from mice with AAV harboring negative

control (AAV-*NC*) or *shAbca1* (AAV- *shAbca1)* at 5-week after injection. (n = 6 for each group). ***P < 0.001 vs. AAV-*NC* mice. **b.** Urinary albumin creatinine ratio in different groups of mice (n = 8 for each group). *P < 0.05, ***P < 0.001 vs. *AAV-NC/Cre*$^{+}$*/Ccdc92*$^{+/+}$ mice, $^{\#\#\#}P$ < 0.001 vs. *AAV-NC/Cre*$^{+}$*/Ccdc92*$^{+/+}$ with STZ/HFD mice, ^{++}P < 0.01 vs. *AAV-NC/Cre*$^{+}$*/Ccdc92*$^{fl/fl}$ with STZ/HFD mice. **c.** Morphological examinations of glomerular changes by Periodic acid–Schiff (PAS) analyses in mice (n = 8 for each group). **P < 0.01, ***P < 0.001 vs. *AAV-NC/Cre*$^{+}$*/Ccdc92*$^{+/+}$ mice, $^{\#\#\#}P$ < 0.001 vs. *AAV-NC/Cre*$^{+}$*/Ccdc92*$^{+/+}$ with STZ/HFD mice, ^{+++}P < 0.001 vs. *AAV-NC/Cre*$^{+}$*/Ccdc92*$^{fl/fl}$ with STZ/HFD mice. **d.** Representative IF images showing the expressions of nephrin and podocin in glomeruli from mice (n = 8 for each group). DAPI (4',6-diamidino-2-phenylindole) was used as a nuclear staining. *P < 0.05, **P < 0.01, ***P < 0.001 vs. *AAV-NC/Cre*$^{+}$*/Ccdc92*$^{+/+}$ mice, $^{\#\#\#}P$ < 0.001 vs. *AAV-NC/Cre*$^{+}$*/Ccdc92*$^{+/+}$ STZ/HFD mice, ^{++}P < 0.01, ^{+++}P < 0.001 vs. *AAV-NC/Cre*$^{+}$*/Ccdc92*$^{fl/fl}$ STZ/HFD mice. **e.** Representative images and quantifications showing lipid deposition by Oil Red O staining and immunofluorescence staining of adipophilin (green) and synaptopodin (red) in kidney from mice (n = 8 for each group). DAPI was used as a nuclear staining. ***P < 0.001 vs. *AAV-NC/Cre*$^{+}$*/Ccdc92*$^{+/+}$ mice, $^{\#\#\#}P$ < 0.001 vs. *AAV-NC/Cre*$^{+}$*/Ccdc92*$^{+/+}$ STZ/HFD mice, ^{+++}P < 0.001 vs. *AAV-NC/Cre*$^{+}$*/Ccdc92*$^{fl/fl}$ STZ/HFD mice. **f.** Representative Nile Red staining images of conditionally immortalized human podocyte cell line with different groups. DAPI was used as a nuclear staining. *si-NC* represents negative control for Ccdc92 knockdown. Data are expressed as mean ± SEM and n indicates the number of biologically independent experiments. Two-tailed Student's unpaired t test analysis (a), Two-way ANOVA followed by Tukey's post-test (b-e).

CCDC92 deficiency ameliorates podocyte lipotoxicity in diabetic kidney disease

CRediT authorship contribution statement

Fuwen Zuo conducted *in vivo* and *in vitro* experiments, performed data analysis, and helped write the manuscript. Youzhao Wang and Xiaojie Wang performed *in vivo* animal studies. Xinlei Xu and Ruihao Ding performed *in vitro* experiments. Wei Tang and Yu Sun analyzed the data. Yan Zhang and Yusheng Xie helped design experiments. Jichao Wu performed the confocal microscopy. Fan Yi, Ziying Wang and Min Liu designed the experiment, interpreted the data, wrote the manuscript, and approved final version of the manuscript for publication.

Graphical abstract

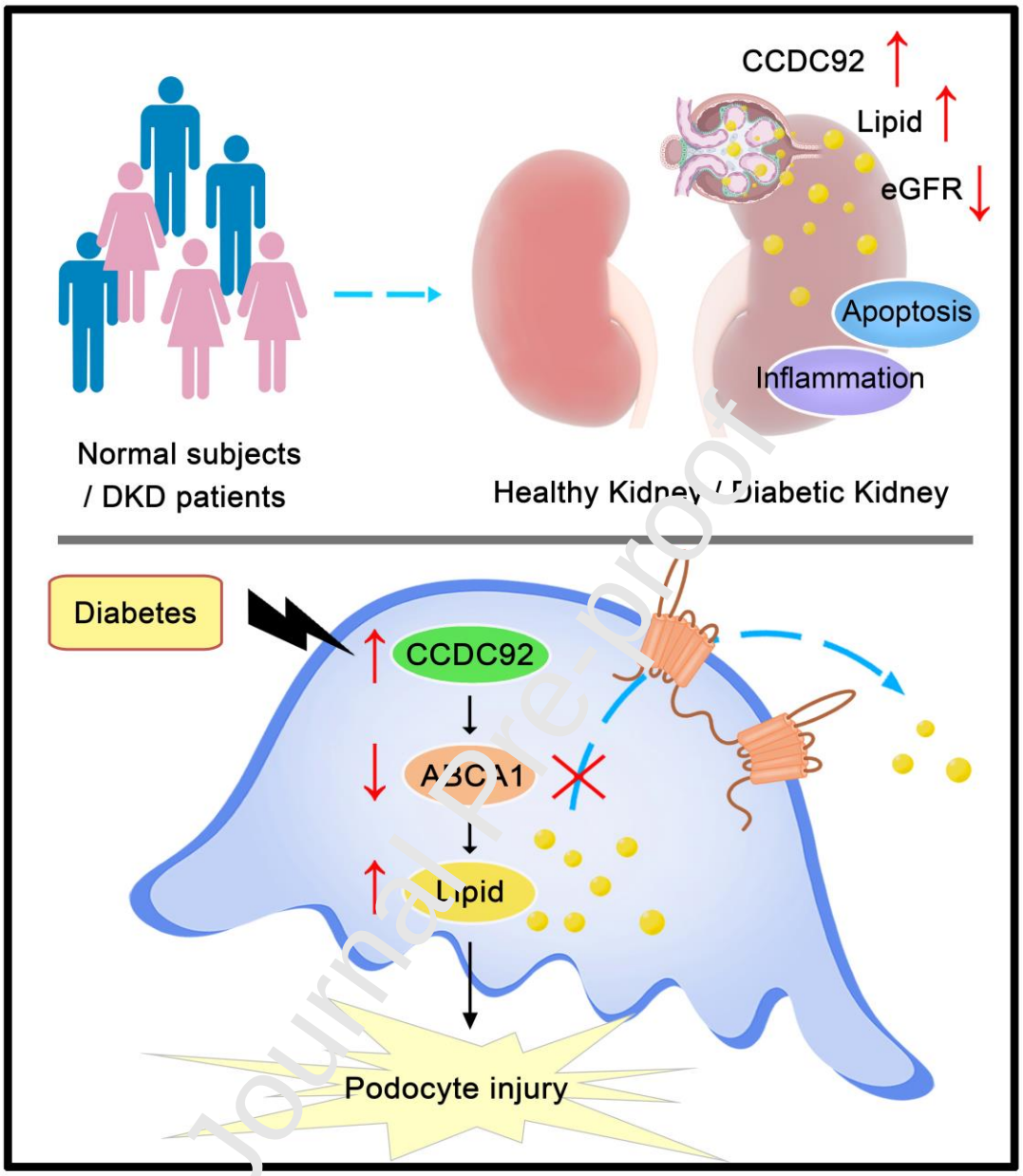

Highlights

1.CCDC92 is increasedin podocytes under diabetic condition.
2. The level of CCDC92in glomeruliis correlated with eGFRand lipid accumulation.
3. Conditional knockout of *Ccdc92*in podocytes ameliorates glomerular injury.
4.CCDC92 contributes to podocyte lipotoxicity in DKD through regulation ofABCA1.

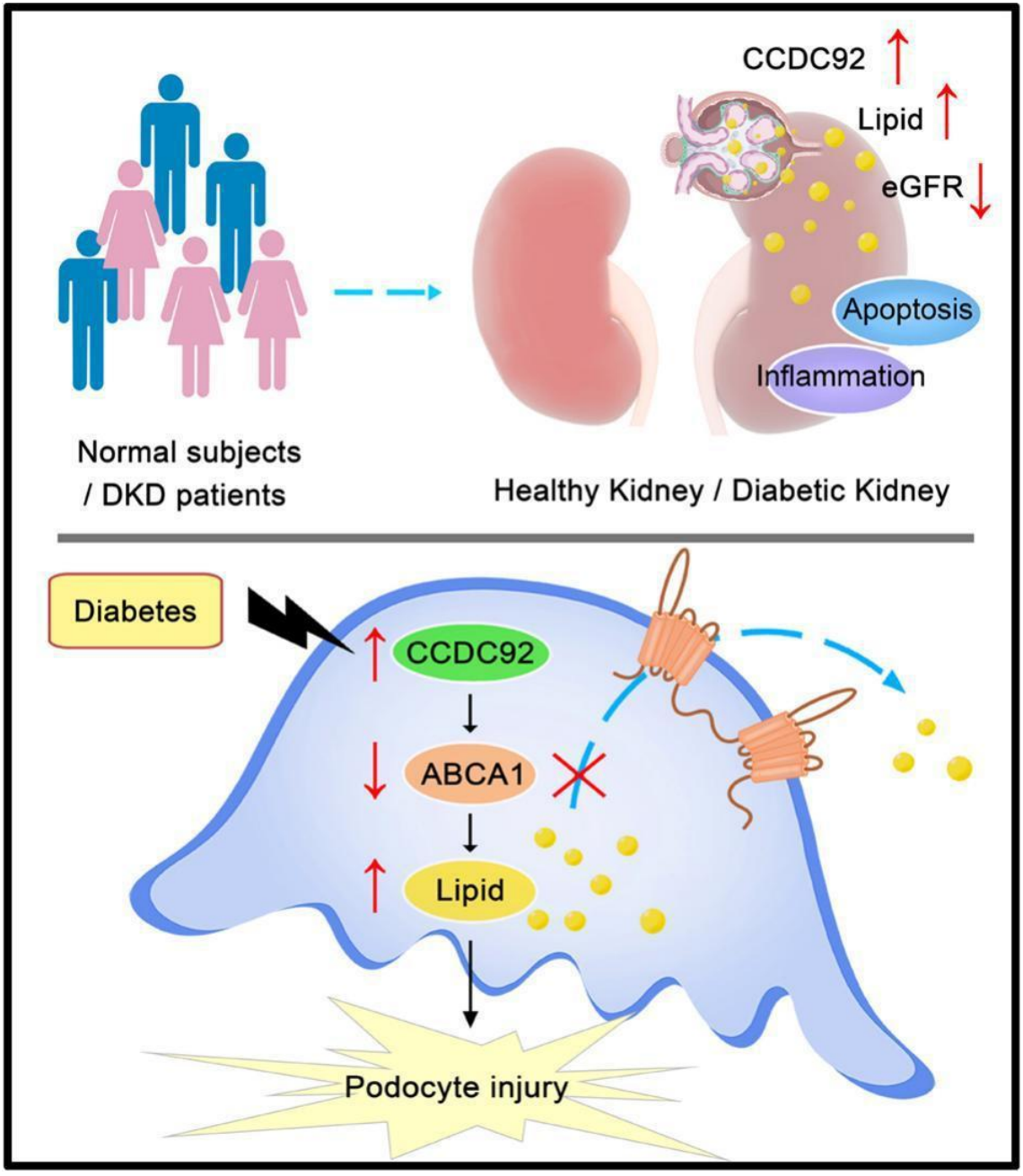

Graphics Abstract

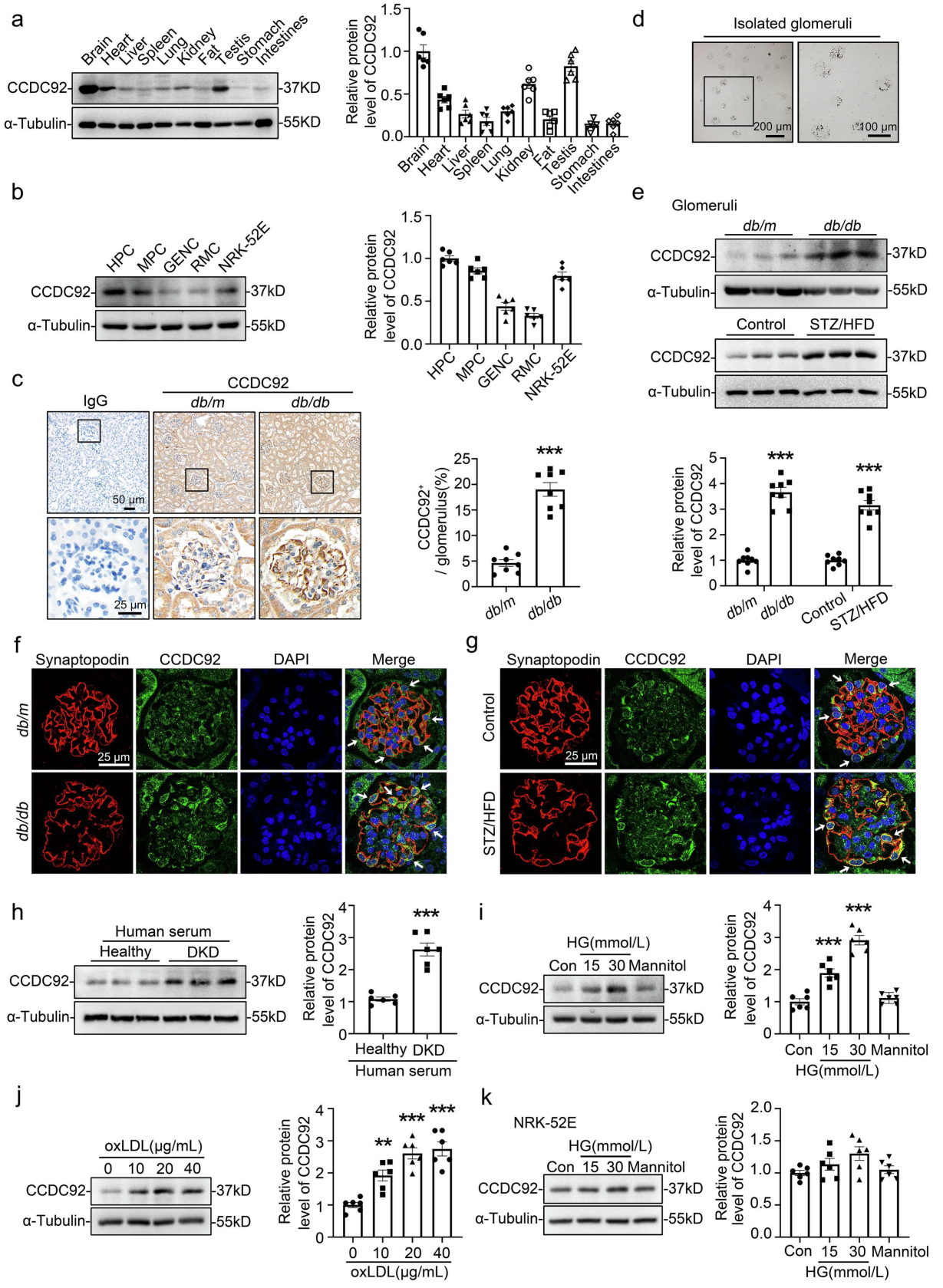
a
Brain
Heart
Liver
Spleen
Lung
Kidney
Fat
Testis
Stomach
Intestines
CCDC92
α-Tubulin
37KD
55KD
Relative protein level of CCDC92
b
HPC
MPC
GENC
RMC
NRK-52E
c
IgG
CCDC92
db/m
db/db
50 μm
25 μm
CCDC92+ / glomerulus(%)
d
Isolated glomeruli
200 μm
100 μm
e
Glomeruli
Control
STZ/HFD
f
Synaptopodin
DAPI
Merge
g
h
Human serum
Healthy
DKD
i
HG(mmol/L)
Con
15
30
Mannitol
j
oxLDL(μg/mL)
0
10
20
40
k
NRK-52E

Figure 1

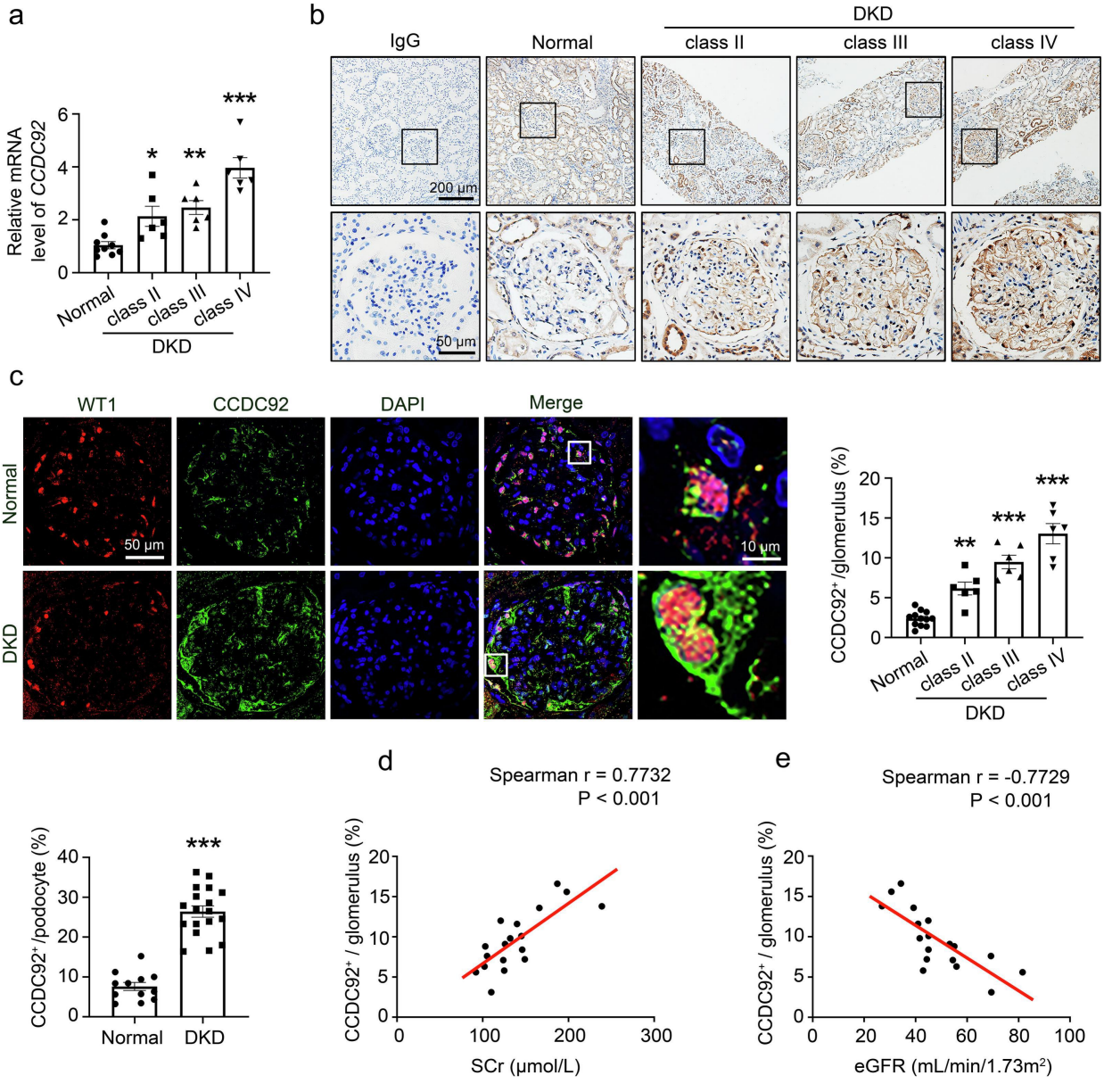
a
Relative mRNA level of CCDC92
Normal
class II
class III
class IV
DKD
b
IgG
Normal
DKD
class II
class III
class IV
200 μm
50 μm
c
WT1
CCDC92
DAPI
Merge
Normal
DKD
50 μm
10 μm
CCDC92+ /glomerulus (%)
CCDC92+ /podocyte (%)
d
Spearman r = 0.7732
P < 0.001
CCDC92+ / glomerulus (%)
SCr (μmol/L)
e
Spearman r = -0.7729
P < 0.001
CCDC92+ / glomerulus (%)
eGFR (mL/min/1.73m2)

Figure 2

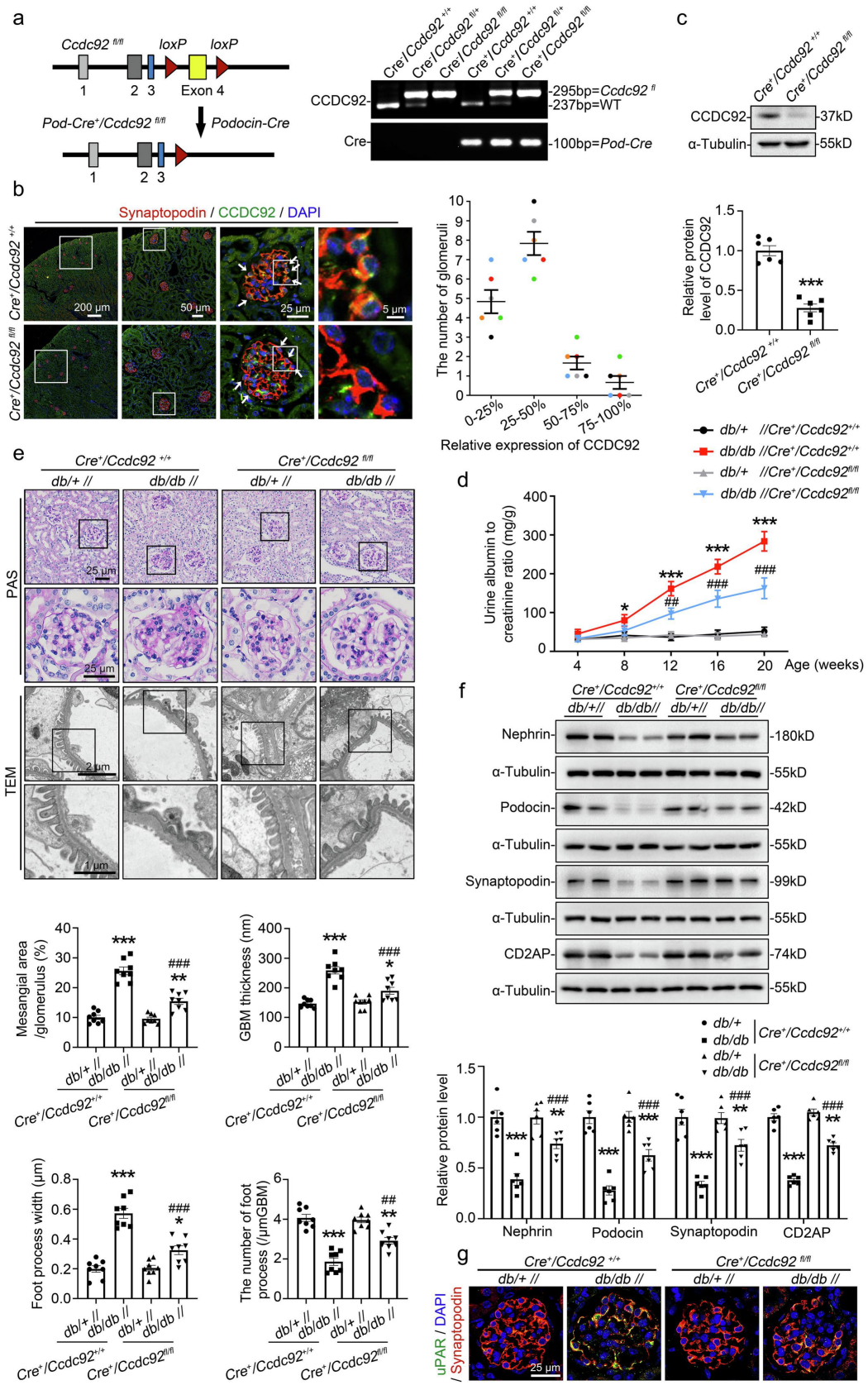
a
Ccdc92 fl/fl
loxP
loxP
1
2 3
Exon 4
Pod-Cre+/Ccdc92 fl/fl
Podocin-Cre
1
2 3
Cre-/Ccdc92 +/+
Cre-/Ccdc92 fl/+
Cre-/Ccdc92 fl/fl
Cre+/Ccdc92 +/+
Cre+/Ccdc92 fl/+
Cre+/Ccdc92 fl/fl
CCDC92-
295bp=Ccdc92 fl
237bp=WT
Cre-
100bp=Pod-Cre
c
Cre+/Ccdc92 +/+
Cre+/Ccdc92 fl/fl
CCDC92-
37kD
α-Tubulin-
55kD
b
Synaptopodin / CCDC92 / DAPI
Cre+/Ccdc92 +/+
Cre+/Ccdc92 fl/fl
200 μm
50 μm
25 μm
5 μm
The number of glomeruli
0-25%
25-50%
50-75%
75-100%
Relative expression of CCDC92
Relative protein level of CCDC92
***
Cre+/Ccdc92 +/+
Cre+/Ccdc92 fl/fl
db/+ //Cre+/Ccdc92+/+
db/db //Cre+/Ccdc92+/+
db/+ //Cre+/Ccdc92fl/fl
db/db //Cre+/Ccdc92fl/fl
e
Cre+/Ccdc92 +/+
Cre+/Ccdc92 fl/fl
db/+ //
db/db //
PAS
TEM
25 μm
2 μm
1 μm
Mesangial area /glomerulus (%)
GBM thickness (nm)
Foot process width (μm)
The number of foot process (/μmGBM)
d
Urine albumin to creatinine ratio (mg/g)
Age (weeks)
f
Cre+/Ccdc92+/+
Cre+/Ccdc92fl/fl
db/+//
db/db//
Nephrin-
180kD
α-Tubulin-
55kD
Podocin-
42kD
Synaptopodin-
99kD
CD2AP-
74kD
Relative protein level
Nephrin
Podocin
Synaptopodin
CD2AP
g
uPAR / DAPI / Synaptopodin
25 μm

Figure 3

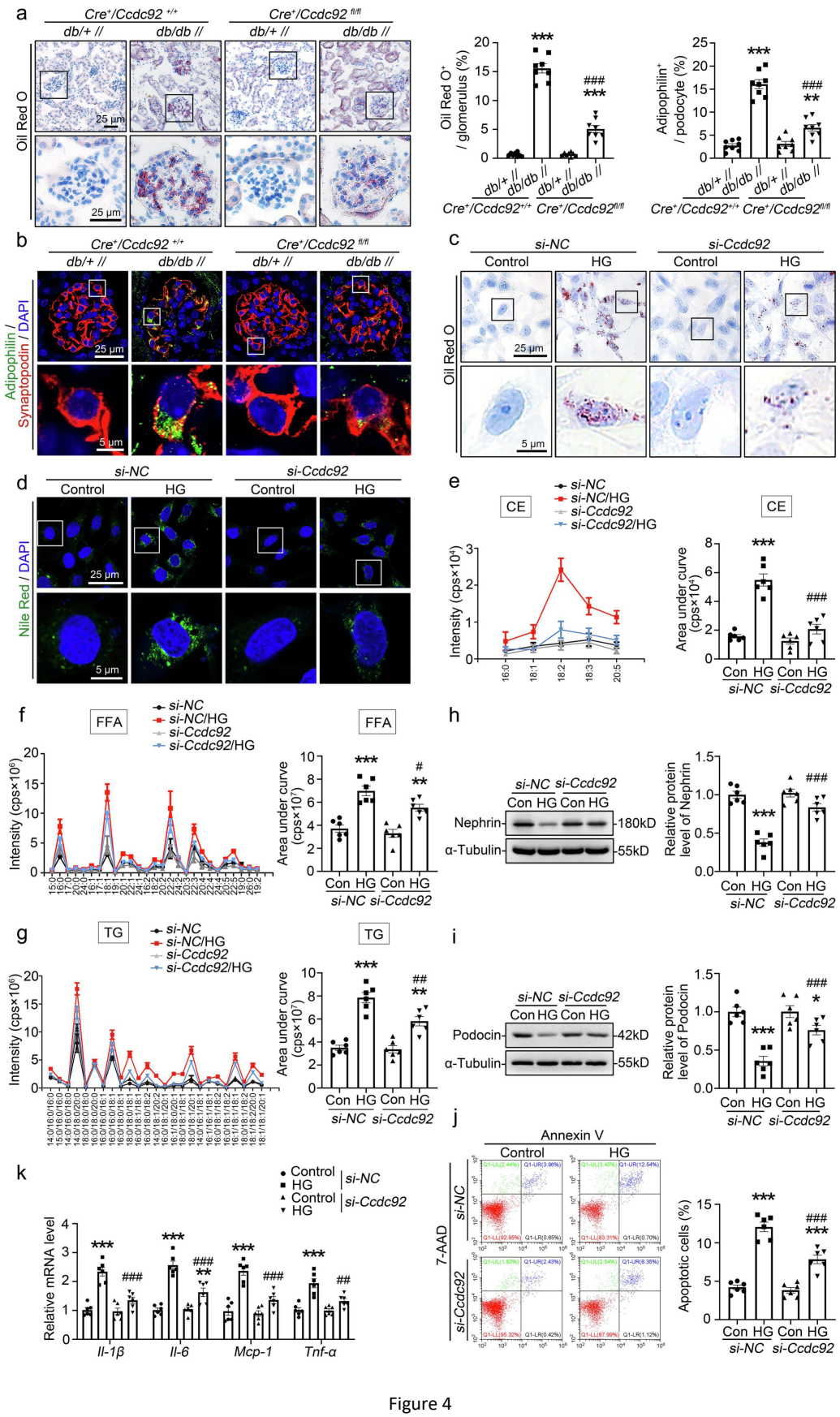
a
Cre+/Ccdc92 +/+
Cre+/Ccdc92 fl/fl
db/+ //
db/db //
Oil Red O
25 μm
Oil Red O+ / glomerulus (%)
Adipophilin+ / podocyte (%)
***
###
**
Cre+/Ccdc92+/+
Cre+/Ccdc92fl/fl
b
Adipophilin / Synaptopodin / DAPI
5 μm
c
si-NC
si-Ccdc92
Control
HG
d
Nile Red / DAPI
e
CE
si-NC
si-NC/HG
si-Ccdc92
si-Ccdc92/HG
Intensity (cps×10⁴)
Area under curve (cps×10⁴)
16:0
18:1
18:2
18:3
20:5
Con
f
FFA
Intensity (cps×10⁶)
Area under curve (cps×10⁷)
#
h
Nephrin
α-Tubulin
180kD
55kD
Relative protein level of Nephrin
g
TG
i
Podocin
42kD
Relative protein level of Podocin
j
Annexin V
7-AAD
Apoptotic cells (%)
k
Relative mRNA level
Il-1β
Il-6
Mcp-1
Tnf-α

Figure 4

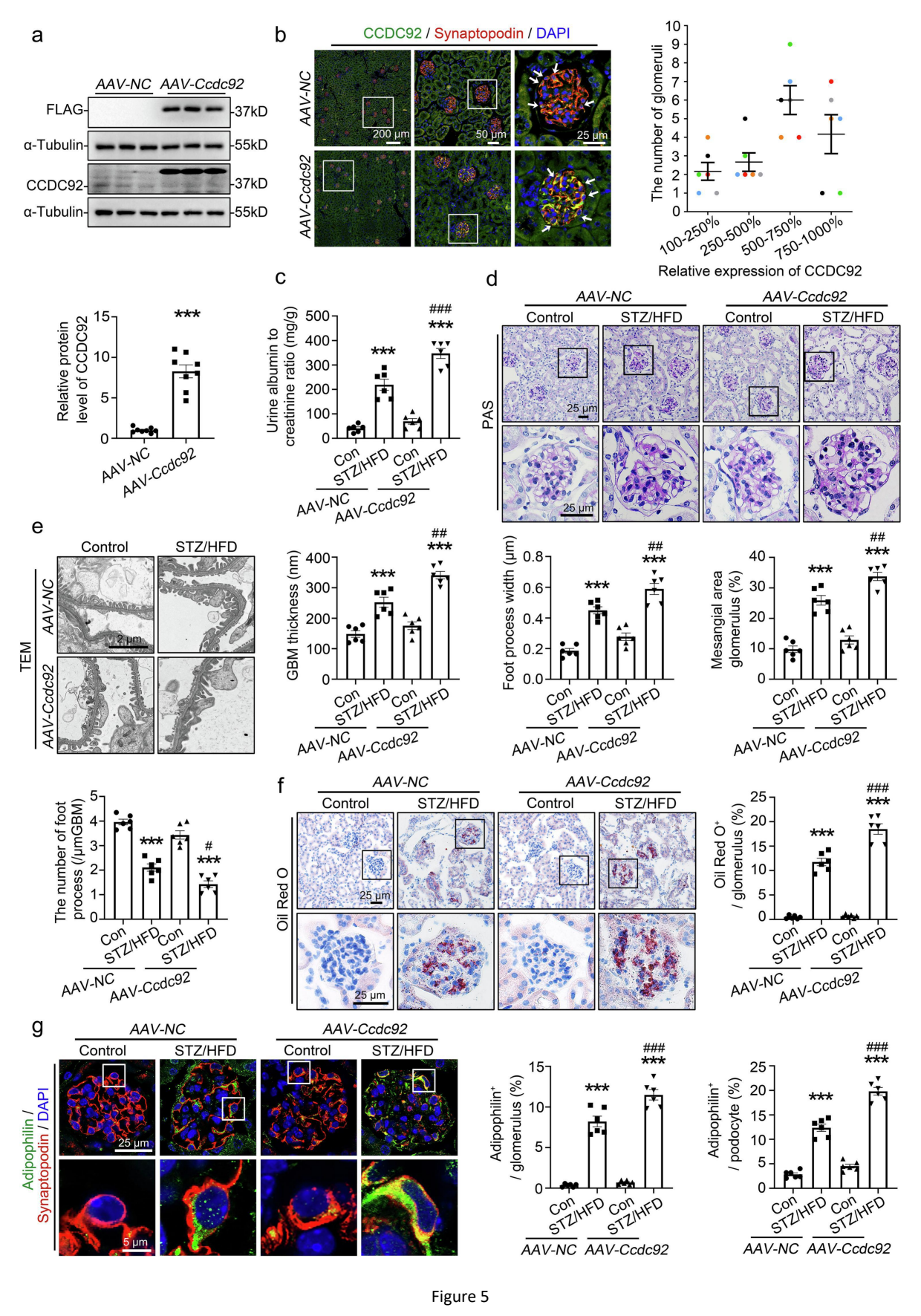
a
AAV-NC
AAV-Ccdc92
FLAG
37kD
α-Tubulin
55kD
CCDC92
37kD
α-Tubulin
55kD
b
CCDC92 / Synaptopodin / DAPI
AAV-NC
AAV-Ccdc92
200 μm
50 μm
25 μm
The number of glomeruli
100-250%
250-500%
500-750%
750-1000%
Relative expression of CCDC92
Relative protein level of CCDC92
AAV-NC
AAV-Ccdc92
c
Urine albumin to creatinine ratio (mg/g)
Con
STZ/HFD
AAV-NC
AAV-Ccdc92
d
AAV-NC
AAV-Ccdc92
Control
STZ/HFD
PAS
25 μm
e
TEM
Control
STZ/HFD
AAV-NC
AAV-Ccdc92
2 μm
GBM thickness (nm)
Foot process width (μm)
Mesangial area glomerulus (%)
The number of foot process (/μmGBM)
f
Oil Red O
25 μm
Oil Red O+ / glomerulus (%)
g
Adipophilin / Synaptopodin / DAPI
25 μm
5 μm
Adipophilin+ / glomerulus (%)
Adipophilin+ / podocyte (%)

Figure 5

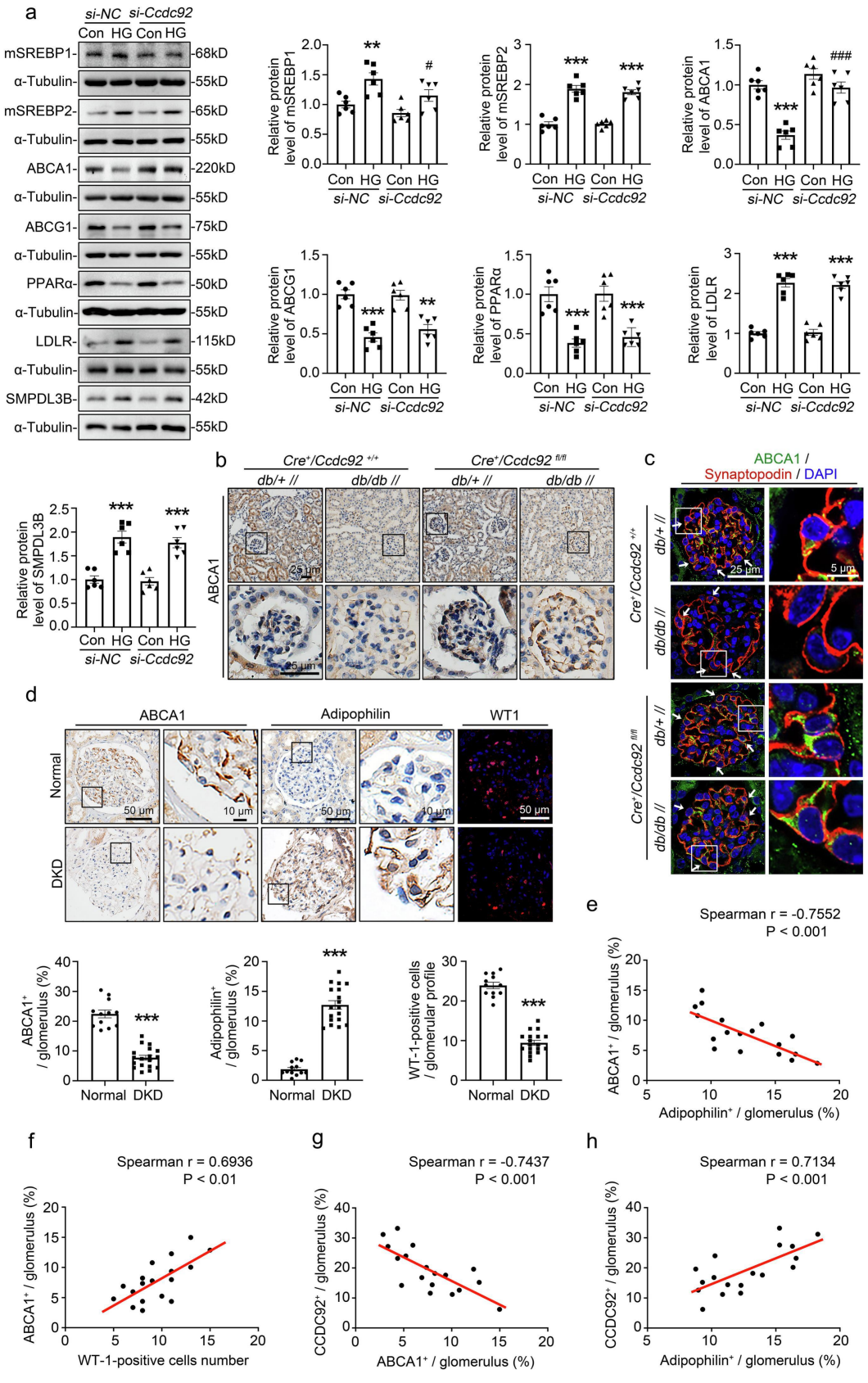
a
si-NC si-Ccdc92
Con HG Con HG
mSREBP1- 68kD
α-Tubulin- 55kD
mSREBP2- 65kD
α-Tubulin- 55kD
ABCA1- 220kD
α-Tubulin- 55kD
ABCG1- 75kD
α-Tubulin- 55kD
PPARα- 50kD
α-Tubulin- 55kD
LDLR- 115kD
α-Tubulin- 55kD
SMPDL3B- 42kD
α-Tubulin- 55kD
Relative protein level of mSREBP1
Relative protein level of mSREBP2
Relative protein level of ABCA1
Relative protein level of ABCG1
Relative protein level of PPARα
Relative protein level of LDLR
Relative protein level of SMPDL3B
Con HG Con HG
si-NC si-Ccdc92
b
Cre+/Ccdc92 +/+
Cre+/Ccdc92 fl/fl
db/+ //
db/db //
ABCA1
25 μm
c
ABCA1 /
Synaptopodin / DAPI
Cre+/Ccdc92 +/+
Cre+/Ccdc92 fl/fl
db/+ //
db/db //
25 μm
5 μm
d
ABCA1
Adipophilin
WT1
Normal
DKD
50 μm
10 μm
ABCA1+ / glomerulus (%)
Adipophilin+ / glomerulus (%)
WT-1-positive cells / glomerular profile
Normal DKD
e
Spearman r = -0.7552
P < 0.001
ABCA1+ / glomerulus (%)
Adipophilin+ / glomerulus (%)
f
Spearman r = 0.6936
P < 0.01
ABCA1+ / glomerulus (%)
WT-1-positive cells number
g
Spearman r = -0.7437
P < 0.001
CCDC92+ / glomerulus (%)
ABCA1+ / glomerulus (%)
h
Spearman r = 0.7134
P < 0.001
CCDC92+ / glomerulus (%)
Adipophilin+ / glomerulus (%)

Figure 6

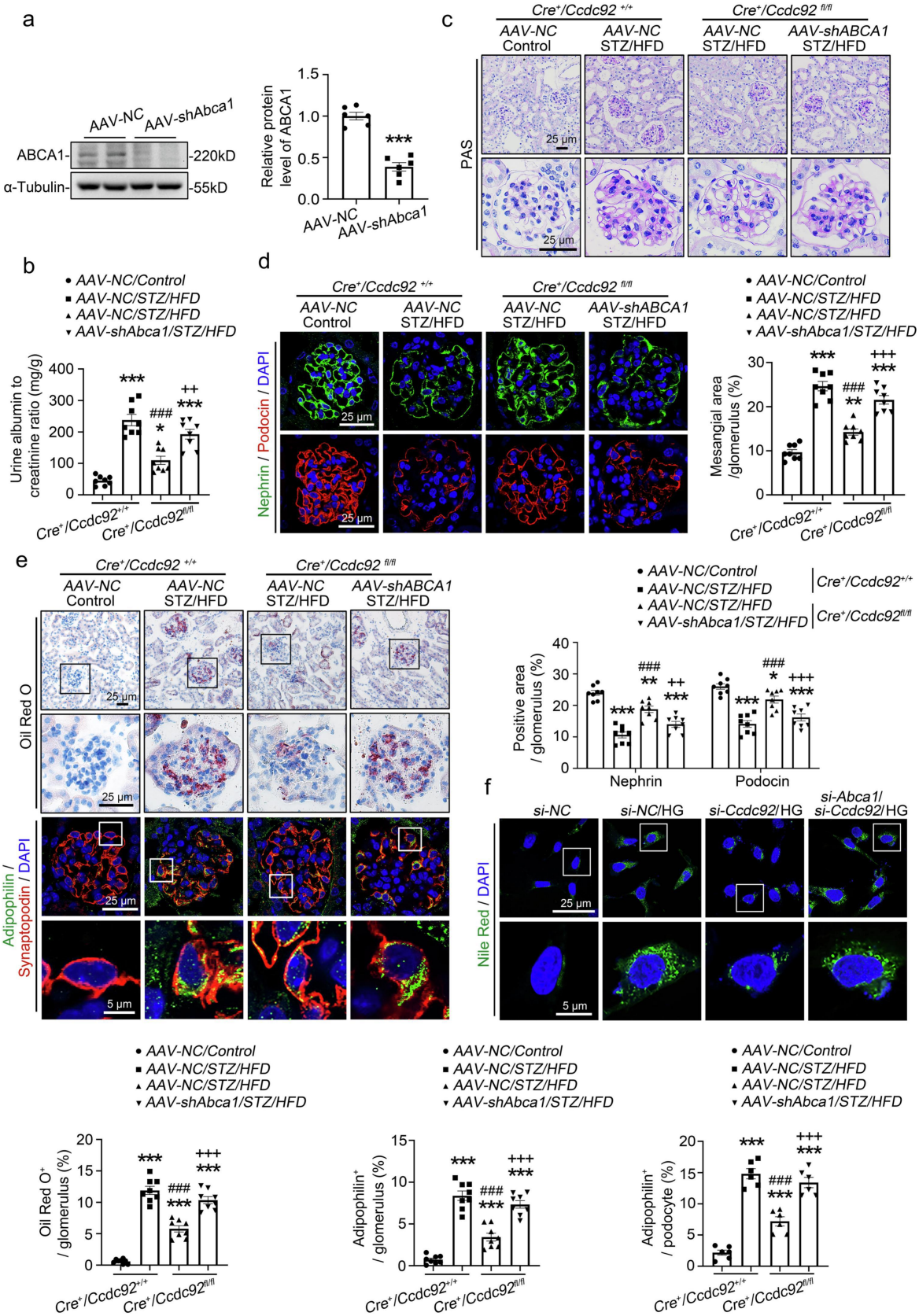
a
AAV-NC
AAV-shAbca1
ABCA1-
-220kD
α-Tubulin-
-55kD
Relative protein level of ABCA1
1.5
1.0
0.5
0.0
***
AAV-NC
AAV-shAbca1
c
Cre+/Ccdc92 +/+
Cre+/Ccdc92 fl/fl
AAV-NC Control
AAV-NC STZ/HFD
AAV-NC STZ/HFD
AAV-shABCA1 STZ/HFD
PAS
25 μm
25 μm
b
AAV-NC/Control
AAV-NC/STZ/HFD
AAV-NC/STZ/HFD
AAV-shAbca1/STZ/HFD
Urine albumin to creatinine ratio (mg/g)
400
300
200
100
0
***
###
*
++
***
Cre+/Ccdc92+/+
Cre+/Ccdc92fl/fl
d
Cre+/Ccdc92 +/+
Cre+/Ccdc92 fl/fl
AAV-NC Control
AAV-NC STZ/HFD
AAV-NC STZ/HFD
AAV-shABCA1 STZ/HFD
Nephrin / Podocin / DAPI
25 μm
25 μm
AAV-NC/Control
AAV-NC/STZ/HFD
AAV-NC/STZ/HFD
AAV-shAbca1/STZ/HFD
Mesangial area /glomerulus (%)
30
20
10
0
***
###
**
+++
***
Cre+/Ccdc92+/+
Cre+/Ccdc92fl/fl
e
Cre+/Ccdc92 +/+
Cre+/Ccdc92 fl/fl
AAV-NC Control
AAV-NC STZ/HFD
AAV-NC STZ/HFD
AAV-shABCA1 STZ/HFD
Oil Red O
25 μm
25 μm
Adipophilin / Synaptopodin / DAPI
25 μm
5 μm
AAV-NC/Control
AAV-NC/STZ/HFD
AAV-NC/STZ/HFD
AAV-shAbca1/STZ/HFD
Cre+/Ccdc92+/+
Cre+/Ccdc92fl/fl
Positive area / glomerulus (%)
40
30
20
10
0
***
###
**
++
***
###
*
+++
***
Nephrin
Podocin
f
si-NC
si-NC/HG
si-Ccdc92/HG
si-Abca1/ si-Ccdc92/HG
Nile Red / DAPI
25 μm
5 μm
AAV-NC/Control
AAV-NC/STZ/HFD
AAV-NC/STZ/HFD
AAV-shAbca1/STZ/HFD
Oil Red O+ / glomerulus (%)
20
15
10
5
0
***
###
***
+++
***
Cre+/Ccdc92+/+
Cre+/Ccdc92fl/fl
AAV-NC/Control
AAV-NC/STZ/HFD
AAV-NC/STZ/HFD
AAV-shAbca1/STZ/HFD
Adipophilin+ / glomerulus (%)
15
10
5
0
***
###
***
+++
***
Cre+/Ccdc92+/+
Cre+/Ccdc92fl/fl
AAV-NC/Control
AAV-NC/STZ/HFD
AAV-NC/STZ/HFD
AAV-shAbca1/STZ/HFD
Adipophilin+ / podocyte (%)
20
15
10
5
0
***
###
***
+++
***
Cre+/Ccdc92+/+
Cre+/Ccdc92fl/fl

Figure 7